

1 se-2013-39

2

3 Submitted on 08 Jul 2013

4

5 The permeability and elastic moduli of tuff from Campi Flegrei, Italy: implications for ground
6 deformation modelling

7

8 M. J. Heap, P. Baud, P. G. Meredith, S. Vinciguerra, and T. Reuschlé

9

10

11 **Dear Antonella Longo,**

12

13 **Firstly, thanks for your time and effort spent in dealing with our submission. In general, we**
14 **are pleased by the positive and constructive nature of the reviewers' comments. The**
15 **comments of the four reviewers are appended below and our responses are given in bold**
16 **below each comment (any changes to the manuscript text is highlight in blue). We believe**
17 **that we have suitably addressed the reviewers' comments and, as a consequence, improved**
18 **our manuscript. We would now like our improved manuscript to be considered for**
19 **publication in *Solid Earth*.**

20

21 **Thank you again for your time.**

22

23 **Yours sincerely,**

24

25 **Mike Heap and co-authors**

26

27 Reviewer #1 (Andrea Manconi)

28
29 The manuscript by Heap et al. presents a systematic laboratory study of the influence of pressure
30 and temperature on the permeability and elastic moduli of the two most widespread tuffs from the
31 Campi Flegrei volcanic district, Italy. Their results show that the water permeability of
32 Neapolitan Yellow Tuff (NYT) and a tuff from the Campanian Ignimbrite (WGI) differ by about two
33 orders of magnitude. In addition, while the NYT properties are systematically affected by
34 temperature, no clear patterns depending on temperatures were revealed for the WGI samples.
35 Moreover, the authors show that the dynamic and static elastic moduli differ significantly.

36
37 The results of this study have implications for surface deformation modelling and interpretation at
38 CF caldera and elsewhere. The manuscript may represent a key contribution for a better
39 understanding the influence of rock physical parameters, as well as for a more conscious use of
40 these parameters in models of deformation processes occurring in active volcanic areas. In some
41 cases, the consideration of homogeneous half-space in mechanical models of deformation processes
42 occurring at volcanic areas might be still acceptable, mainly because of lack of information on the
43 material properties. However, in cases as CF caldera where a large dataset of information is already
44 present, the effect of heterogeneities has to be taken carefully into account. Instead, if homogeneous
45 half space is still preferred in modeling attempts, one has to be aware that this might be an
46 oversimplification deeply influencing the modeling results and thus potentially leading to
47 misinterpretations. The methodology and results are clearly presented and thoroughly discussed in
48 the manuscript. Due to the high quality of the results and their important implications, the paper
49 deserves publication in Solid Earth, though some very minor issues have to be clarified before final
50 acceptance. Please find my specific comments/criticism here below.

51
52 **We are pleased that reviewer #1 considers the manuscript a “key contribution for a better
53 understanding the influence of rock physical parameters, as well as for a more conscious use
54 of these parameters in models of deformation processes occurring in active volcanic areas”
55 and that our results are of a “high quality” with “important implications”.**

56
57 1) Please provide and eventually discuss/comment expected errors in the estimation of rock
58 properties for the considered methodologies of investigation. This might help the reader to better
59 evaluate the results of your analyses.

60
61 **This is certainly an important consideration in experimental work. However, commonly, the
62 measurement error is insignificant when compared with the natural variability of samples
63 cored from the same block (even for “well-behaved” sandstone or granite samples). We have
64 now added the following paragraph and two new tables, one showing the measurement
65 accuracy and one showing the expected natural sample variability:**

66
67 **“Experimental data are subject to error as a result of the accuracy of the various
68 transducers. Estimations of the accuracy of the measurements of this study are listed in
69 Table 2. The errors are extremely small and lead to error bars that are smaller than the data**

70 points in the figures provided in this study. However, we note that measurement error is
71 dwarfed by the natural sample variability of the tuffs (i.e., the natural variability of samples
72 cored from the same block of material). Estimations of the natural sample variability of the
73 tuffs used this study are provided in Table 3.”

74
75
76 **Table 2. Summary of the estimated measurement accuracy.**

measurement	accuracy
confining pressure [Pa]	$\pm 100\,000$ (UCL) $\pm 10\,000$ (Strasbourg)
pore fluid pressure [Pa]	$\pm 10\,000$
pore fluid volume [m^3]	$\pm 1.0 \times 10^{-12}$
LVDT displacement [m]	± 0.000001
axial stress [Pa]	$\pm 10\,000$
original sample dimensions [m]	± 0.00001

77
78
79 **Table 3. Expected natural variability between tuff samples cored from the same block. Note**
80 **that these are not “errors” in the measurements. Measurement accuracies (Table 2) are**
81 **insignificant compared to the natural sample variability, despite efforts to reduce the**
82 **variability between samples cored from the same block of material (see text for details).**

	expected natural variability
Young's modulus [GPa]	± 0.5
Poisson's ratio	± 0.05
shear modulus [GPa]	± 0.5
water permeability [m^2]	$\pm 1.0 \times 10^{-14}$
P-wave velocity [km s^{-1}]	± 0.1
S-wave velocity [km s^{-1}]	± 0.1

83
84
85 2) In section 5.3, the authors claim that the NYT and WGI have similar elastic moduli, (thought
86 pressure/depth dependent) supporting the homogeneous half space notion for the CF caldera.
87 However, this statement might be misleading, as these rocks represent only a portion of the caldera
88 infill materials (see e.g. Orsi et al., JVGR 1996).

89
90 **The reviewer is correct. In fact, those data do not support the notion of a homogenous half**
91 **space model. We have now completely reworded this paragraph:**

92
93 **“Our data highlight that the elastic moduli of two different tuffs from CF are significantly**
94 **depth-dependent (Figures 7 and 8). The implication of these data is that the assumption of a**
95 **homogenous half-space may be an oversimplification, and is exacerbated further when one**
96 **considers the extent of the variability of the tuffs within the caldera (which are variably**
97 **lithified, altered, and zeolitized, see the report of Giberti et al., 2006). These data highlight**

98 the need for the development of more complex, multi-layer ground deformation models. In
99 order to assess the extent of the variability in elastic moduli of the rocks within the caldera
100 at CF, a systematic experimental approach involving borehole samples from different depths
101 and locations within the caldera is now required (discussed further at the end of the
102 section)."

103

104 3) Fig. 4 is the only one among figs 4-7 where the effective pressure is on the y-axis. Then figs. 8-9
105 show the differential stress on y-axis. I suggest to make all figures consistent (e.g. pressure/stress
106 on the x-axis for all figures, or vice-versa) to ease their reading and eventual cross-comparison.

107

108 The reviewer is correct in the fact that effective pressure is on the y-axis of Figure 4 and is on
109 the x-axes of Figures 5-7; and that differential stress is on the y-axes of Figures 8 and 9. The
110 reason for this is that this is how these data are most commonly portrayed in the wealth of
111 previous literature. While we agree that there is some merit in organising them as the
112 reviewer suggested, we would prefer to keep our figures in the standard format.

113

114 4) Please check that abbreviations are systematically defined when used for the first time in the
115 text. I could not find the definition for Pp.

116

117 The reviewer is correct. We have now amended this: "Once inside the setup, the confining
118 pressure (Pc) and the pore fluid (distilled water) pressures (Pp) in both the "upstream" (P_{up})
119 and "downstream" (P_{down}) pore volumometers were increased to 10 and 5 MPa,
120 respectively."

121

122 Reviewer #2 (Claudia Cannatelli)

123

124 The manuscript by Heap and coauthors presents an experimental study of the effect that pressure
125 and temperature have on permeability and elastic moduli of CI and NYT at Campi Flegrei, Italy.
126 Their results show that the water permeability of Neapolitan Yellow Tuff (NYT) and a tuff from the
127 Campanian Ignimbrite (WGI) differ by about two orders of magnitude, indicating an heterogeneous
128 nature of Campi Flegrei's tuffs. They also point out how the permeability and the elastic moduli of
129 NYT is affected by thermal stressing increase, while the CI appears not to be affected by such stress.
130 The manuscript is well written; the methodology and results are well presented and discussed in
131 the manuscript. The results are very important for the understanding of how the physical
132 parameters of the rock can affect processes such the bradyseism at Campi Flegrei. The bibliography
133 on the Campi Flegrei is outdated, and therefore the presentation of the geological background lacks
134 the most recent published papers (last 10 years!) on the topic. I would recommend publication of
135 this manuscript, but revision of the introduction is NEEDED in order to have an updated description
136 of the volcanic area and its products. In specific, here are my comments:

137

138 **We are pleased that reviewer #2 deems our results as “very important for the understanding**
139 **of how the physical parameters of the rock can affect processes such the bradyseism at**
140 **Campi Flegrei.” We have now improved our introduction section, which now boasts a more**
141 **up-to-date reference list (see our answers to the below comments).**

142

143 Line 69-70 The Neapolitan area is surrounded by Mt. Somma-Vesuvius to the east and the Campi
144 Flegrei volcanic system to the west. So I will suggest the authors to change Line 69-70 with the
145 following sentence: “The densely populated (about 3 million) Neapolitan area, southern Italy, is in a
146 state of constant threat provided by the proximity of Mt. Somma-Vesuvius and Campi Flegrei (CF)
147 volcanic district.”

148

149 **Agreed. This has now been changed:**

150

151 **“The densely populated (about 3 million) Neapolitan area, southern Italy, is in a state of**
152 **constant threat provided by the proximity of Mt. Vesuvius and the increasingly-restless**
153 **Campi Flegrei (CF) volcanic district (Ricci et al., 2013; Figure 1).”**

154

155 Line 72-73 There are several theories around the activity at Campi Flegrei, which are not taken into
156 account by the authors. Also the bibliography they use is very old (almost 10 years old) and lot of
157 new data has been produced since 1999. As far as the activity in CF, some authors (Rosi and Sbrana,
158 1987; Orsi et al., 1996) relate the origin of Campi Flegrei either to the eruption of the Campanian
159 Ignimbrite (CI, 39 ka, De Vivo et al., 2001), or to the Neapolitan Yellow Tuff (NYT, 15 ka, Deino et al.,
160 2004). Other authors (De Vivo et al., 2001; Rolandi et al., 2003) interpret the eruption of the CI not
161 as a unique event originating in the Campi Flegrei caldera, but as a sequence of eruptive events
162 occurred from fractures activated along the neotectonic Apennine fault system parallel to the
163 Tyrrhenian coastline. These events, of ignimbritic origin, lasted from >300 ka to 19 ka and are not

164 confined to a unique volcanic center in Campi Flegrei. According to Rolandi et al. (2003), only the
165 NYT erupted within Campi Flegrei, whereas the CI has a much wider source area.

166

167 **Based on these suggestions, we have now significantly improved this paragraph. Notably, we**
168 **have: (1) included more up-to-date references and, (2) discussed both hypotheses for the**
169 **eruption of the Campanian Ignimbrite. The text is now as follows:**

170

171 **"The eruptive history of the CF volcanic district can be characterised by two major**
172 **eruptions: (1) the eruption related to the emplacement of the Campanian Ignimbrite about**
173 **39,000 years ago (De Vivo et al., 2001) and, (2) the eruption of the Neapolitan Yellow Tuff**
174 **(NYT) about 15,000 years ago (Deino et al., 2004); although the area has been volcanically**
175 **active for more than 300,000 years (Rolandi et al., 2003). Today, the CF volcanic district is**
176 **dominated by a resurgent, nested caldera (Figure 1) that hosts a large, shallow (< 4 km)**
177 **hydrothermal system (e.g., De Natale et al., 2006). The CF caldera is considered to have**
178 **formed due to collapse following (1) both of the major eruptions (e.g., Barberi et al., 1991;**
179 **Orsi et al., 1996) or, (2) the eruption of the NYT only (see Rolandi et al., 2003 and references**
180 **therein). In the latter hypothesis, the Campanian Ignimbrite is thought to be the result of**
181 **eruptive events originating from pre-existing neotectonic faults formed during the Apennine**
182 **uplift (De Vivo et al., 2001; Rolandi et al., 2003)."**

183

184 Line 74 It is well established that the Campanian Ignimbrite (CI) is dated at 39ka (De Vivo et al.,
185 2001) and the Neapolitan Yellow Tuff (NYT) at 15ka (Deino et al., 2004).

186

187 **Agreed. The text now reads:**

188

189 **"The eruptive history of the CF volcanic district can be characterised by two major**
190 **eruptions: (1) the eruption related to the Campanian Ignimbrite about 39,000 years ago (De**
191 **Vivo et al., 2001) and, (2) the eruption of the Neapolitan Yellow Tuff (NYT) about 15,000**
192 **years ago (Deino et al., 2004); although the area has been volcanically active for more than**
193 **300,000 years (Rolandi et al., 2003)."**

194

195 Line 84-98 This is just according with one source!! What about the other proposed models? Why
196 the authors choose Chiodini's model over all the others? Why the authors prefer this model to the
197 others published? It seems that the model from Chiodini et al is the one explaining the bradyseismc
198 events in CF, while the others are only specualtions. I would suggest the authors to rephrase the
199 sentences in lines 84- 98 and to list ALL the proposed models for ground deformation at CF.

200

201 **Our goal was never to review and critically appraise the various models proposed to explain**
202 **ground deformation at CF. However, we agree that the paragraph could be improved to**
203 **better explain the various models, and to remove any hint of unintentional bias. The**
204 **paragraph now reads:**

205

206 "However, the interpretation of long-term and short-term ground deformation patterns at
207 CF is a matter of debate (see De Natale *et al.*, 2001 and De Natale *et al.*, 2006 for reviews on
208 the topic). Models to explain the origin of the uplift can be broadly divided into two camps:
209 those that consider solely the input of magma at depth (e.g., Berrino *et al.*, 1984; Bonafede *et*
210 *al.*, 1986; Bianchi *et al.*, 1987) and those that invoke an interaction between magma and
211 fluids (magmatic-hydrothermal models and thermodynamic models; e.g., Bonafede, 1991;
212 Gaeta *et al.*, 1998; Bonafede and Mazzanti, 1998; De Natale *et al.*, 2001; Lundgren *et al.*, 2001;
213 Troise *et al.*, 2001; Gaeta *et al.*, 2003; Chiodini *et al.*, 2003; Battaglia *et al.*, 2006; Gottsmann
214 *et al.*, 2006; Troise *et al.*, 2007; Bodnar *et al.*, 2007; Lima *et al.*, 2009; Todesco *et al.*, 2010;
215 D'Auria *et al.*, 2011; Troiano *et al.*, 2011; Chiodini *et al.*, 2012). The latter category can be
216 broken down further into models that require the input of fresh magma from depth (e.g.,
217 Gaeta *et al.*, 1998) and those that consider magma body cooling and concomitant
218 crystallisation (e.g., Bodnar *et al.*, 2007; Lima *et al.*, 2009). Other models account for the
219 surface deformation by invoking an interaction between the pressure source and caldera
220 boundary fractures (e.g., De Natale and Pingue, 1993; Beauducel *et al.*, 2004) or mechanical
221 heterogeneities (e.g., Manconi *et al.*, 2010). While we note that the goal of this contribution is
222 not to critically review the numerous models invoked to explain the ground deformation at
223 CF, we highlight that the accuracy of all these models relies on accuracy of the rock physical
224 property input parameters. Unfortunately, published laboratory investigations on the
225 physical properties of representative materials from the CF caldera are rare..."
226

227 Line 94 Lima *et al.* (2009) present a quantitative model for subsidence and uplift, based on the
228 linkage between bradyseism and magma body cooling and concomitant crystallization and fluid
229 phase exsolution, coupling long timescale magma crystallization and volatile exsolution from melt
230 and expulsion from magma to shorter timescale hydrothermal system behavior.

231 **We now discuss this in the text:**

232 "The latter category can be broken down further into models that require the input of fresh
233 magma from depth (e.g., Gaeta *et al.*, 1998) and those that consider magma body cooling and
234 concomitant crystallisation (e.g., Bodnar *et al.*, 2007; Lima *et al.*, 2009)."

235 Line 149 CI and NYT are NOT the two major eruption in CF. The authors are speculating that CI has
236 occurred in the CF, while several authors suggested (in several articles, that the authors are
237 ignoring) that it occurred OUTSIDE the CF. Furthermore, the ages attributed to the eruptions are
238 outdated. Again, CI occurred 39 ka (De Vivo *et al.*, 2001) and NYT occurred 15Ka (Deino *et al.*,
239 2004).

240 **We have now changed the wording of this paragraph:**

241 "Our experiments were performed on samples of Neapolitan Yellow Tuff (NYT) and grey
242 Campanian Ignimbrite (WGI), sampled from the two most abundant and widespread
243 volcanic deposits in the CF volcanic district."

249
250 Line 359 Make reference with figure, example Fig. 6A. Apply to all the properties you discuss: S-
251 wave -Figure 6B, Young modulus -figure 6C and so on.
252
253 We have now included references to each specific figure panel in the text.
254
255 Line 362 Add A-F. General comment: since you have labeled the figure A through F, you should
256 somehow report the same labeling in the text.
257
258 We have now included references to each specific figure panel in the text.
259
260 Line 364 Add A-F. See comment for figure 6.
261
262 We have now included references to each specific figure panel in the text.
263
264 Line 366 Make reference to figure, labeling each property with the appropriate letter.
265
266 We have now included references to each specific figure panel in the text.
267
268 Line 374 Add A-B
269
270 We have now included references to each specific figure panel in the text.
271
272 Line 432 Figure 10 is composed by 3 SEM photos, which are not explained at all in the text. In
273 particular what is figure 10A represent? From the figure caption is clear that C is a zoom of B, but
274 what is A?
275
**276 Figure 10 (now Figure 11) simply shows evidence for pore collapse in NYT. We do not think
277 that the figure warrants a lengthy description. We think that our current description in the
278 text is sufficient:**
279
**280 "Evidence of pore collapse is illustrated in the E-SEM image of a sample of NYT taken beyond
281 P* provided as Figure 11."**
282
**283 However, we agree that we do not explain what is shown in panel A. We have now changed
284 the text in the figure caption to read:**
285
**286 "Figure 11. Scanning electron microscope images of an as-collected sample of Neapolitan
287 Yellow Tuff taken beyond P*. **Panel A shows an overview of the post-P* microstructure at a
288 low magnification. Panels B and C show detailed evidence of pore collapse (indicated by the
289 white arrows). Panel C is a zoom of the white box shown in panel B."****
290

291 Line 452 A-C. Description of figure? Why there are no pictures to compare WGI before and after the
292 heating?

293

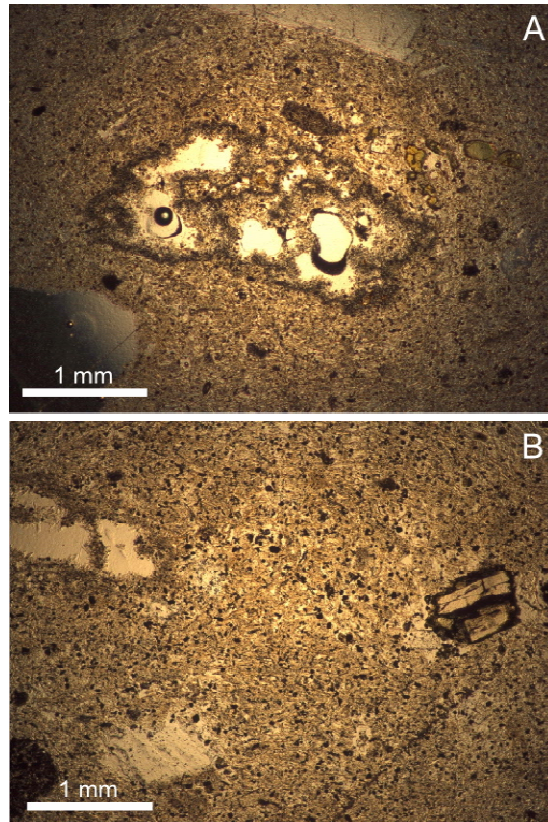
294 **We have now included a new figure (Figure 13, see below) that shows photomicrographs of a**
295 **sample of WGI heated to 1000 °C, and new text describing both Figures 12 and 13:**

296

297 **"Optical microscope photomicrographs of NYT and WGI thermally stressed to a temperature**
298 **of 1000 °C are provided as Figures 12 and 13, respectively. Figure 12 shows that the**
299 **microstructure of NYT is very different to that depicted in Figure 2B for the as-collected**
300 **material. Many cracks are present (Figure 12A, B and C) and some areas contain 1 mm wide**
301 **foamed glass (Figure 12A). By contrast, the microstructure of WGI, upon exposure to 1000 °C**
302 **(Figure 13), is indistinguishable from the as-collected microstructure shown in Figure 2D.**
303 **These observations have been previously reported in Heap *et al.* (2012)."**

304

305



306
307 **Figure 13. Optical microscope images of grey Campanian Ignimbrite thermally stressed to a**
308 **temperature of 1000 °C. Both photographs are taken from Heap *et al.* (2012).**

309

310

311 Line 456 Which ones? Reference such studies!

312

313 **We have now included a reference:**

314 "Detailed studies (de Gennaro and Colella, 1989 and references therein) on the thermal
315 decomposition of the zeolites in NYT have highlighted that analcime loses water
316 irreversibly..."

317

318 Line 458 "chabazite and phillipsite undergo a partial reversible dehydration at 240 °C". Reference??

319

320 **See our answer to the above comment.**

321

322 Line 506-509 Some parentheses are missing. Please check!

323

324 **This has now been amended.**

325

326 Line 519-520 why do you use ONLY this model??? There are 4-5 other models for the bradyseismic
327 events at CF. Why assuming that this one is the right one?? Explain why this model is better than
328 the others!!

329

330 **As stated above, our goal was never to critically appraise the various ground deformation
331 models. We aim to provide values for, and discussion on, experimentally determined values
332 of elastic moduli and permeability (in the sentence in question we are discussing
333 permeability). However, we appreciate that we could word the sentence to sound a little less
334 biased. We have now reworded the sentence to:**

335

336 **"To date, the values of permeability used in the numerous thermodynamical and magmatic-
337 hydrothermal models have spanned many orders of magnitude. For example..."**

338

339 Line 537-539 What will be the difference between samples collected in boreholes from different
340 parts of the caldera and those available from the AGIP survey? Wouldn't the sample be compacted
341 as well? I do not understand the NEED to have more boreholes in the CF caldera, if the samples are
342 going to be affected by the same "problems" of those from AGIP boreholes. Please explain the
343 reasons why there is the need of collecting both.

344

345 **The tuffs comprising the caldera are expected to be heterogeneous both vertically and
346 laterally. The AGIP boreholes are a great place to start, but were drilled at the edges of the
347 caldera. While the level of compaction may be comparable, temperatures are likely to be
348 higher in the centre of the caldera, and the rocks exist within the hydrothermal system.
349 Therefore, thermo-metamorphism/alteration is likely to be more prevalent in the centre of
350 the caldera. To best understand the extent of the variation, both AGIP samples and samples
351 from new, more central boreholes would be ideal (although we are aware that is easier said
352 than done!). In an attempt to be clearer, we have changed the wording of this sentence:**

353

354 **"It is clear that systematic measurements on deep scientific borehole samples are now
355 needed from multiple locations and depths within the caldera to assess the extent of the
356 variability in static elastic moduli and permeability of the rocks that form the caldera."**

357 Reviewer #3 (Maurizio de' Gennaro)

358

359 I carefully read the paper titled "The permeability and elastic moduli of tuff from Campi Flegrei..."
360 also because I know one of the Authors so, I wanted to deepen the review as much as possible,
361 always within my own specific competencies.

362

363 I cannot hide my perplexities on the scientific value of the paper as the objective of the Authors is
364 the drawing of a model that can foresee and interpret the reasons of the soil deformations in Campi
365 Flegrei, by means of laboratory data carried out on outcropping pyroclastic rock samples.

366

367 **The authors find this comment very strange: we do not present a model in our manuscript.**
368 **Our aim was to provide new data to improve the accuracy of the various pre-existing models.**
369 **We are now more explicit about this point:**

370

371 **...While we note that the goal of this contribution is not to critically review the numerous**
372 **models invoked to explain the ground deformation at CF, we highlight that the accuracy of all**
373 **these models relies on accuracy of the rock physical property input parameters..."**

374

375 As you can note by the comments within the text the Authors evidence a very scarce knowledge of
376 the most recent data (the radiometric data of NYT and WGI are not those from a recent literature).
377 Also, they do not cite a paper from Lima et al. (2009) – Earth Science Reviews, which contain a
378 detailed model of the Campi Flegrei underground as well as a different hypothesis concerning the
379 causes of bradyseism. This aspect could even invalidate their model.

380

381 **We appreciate that we should have been more up-to-date with our referencing. Thanks to**
382 **the comments of reviewers #2 and #3, we think we have now suitable addressed this**
383 **problem (see our answers above). We now also discuss the findings of Lima et al. (2009).**
384 **However, as outlined above, we do not present a model to explain ground deformation at CF.**

385

386 The most puzzling aspects are hereafter shortly reported:

387

388 1 The authors use the term tuff as a lithological term, but they have to clarify the concept before the
389 first use. They have to point out that they are considering a tuff as a pyroclastic rock lithified owing
390 to post depositional processes. As a matter of fact, the usage they make of the word tuff should be
391 avoided, because the meaning is confusing: better to use a lithified pyroclastic rock.

392

393 **In our experience, the materials used in this study are well known and well documented in**
394 **the scientific literature as "tuffs". We note that reviewers #1 and #2, who have both worked**
395 **on Campi Flegrei, were happy with our use of the word "tuff". However, we now refrain from**
396 **calling the rocks "tuffs" until our use of the term is defined in the methods section: "In this**
397 **paper we refer to both lithified pyroclastic rocks as "tuffs". We have also changed a**
398 **sentence in the abstract: "...the two most widespread lithified pyroclastic rocks from the**
399 **Campi Flegrei volcanic district, Italy. Our data..."**

400 2 Laboratory tests carried out on very small specimens of such a high heterogeneous material is a
401 shadow on the reliability of the results. The Authors do not report the number of specimens used
402 for each test. Is that a mean value? Not reported. The amount of lithics, pumice, matrix strongly
403 affects the physical and mechanical behavior of the rock and in such a small specimen as those used
404 by the Author, you can find prevailing matrix vs. pumices and vice versa with values completely
405 different.

406
407 We agree that our experimental samples are relatively small when compared with the
408 natural deposit. This is an inherent problem with experimental studies. There is little we can
409 do to circumvent this problem: we cannot measure the permeability/strength of extremely
410 large samples. However, since little is known as to the permeability of these materials, we
411 would argue that our measurements still offer some valuable insight. Further, a report by
412 Giberti et al. (2006) show that 12 and 125 cm³ samples of a variety of rocks from CF have
413 very similar porosities. We have now added a sentence in the "materials investigated"
414 section to highlight these data:

415
416 "We note that, although our samples are small compared to the volume of the natural
417 deposits, a report by Giberti et al. (2006) showed that the porosity of 12 cm³ and 125 cm³
418 samples were very similar, for a wide range of material from CF."

419
420 We performed one experiment per condition: our permeability data (a total of 130
421 permeability measurements) do not represent mean values. However, in an attempt to
422 minimise sample variability, all of the samples were cored from the same block and in the
423 same direction. Any anomalous samples (i.e., those containing large crystals, clasts, or
424 pumice lapilli) were removed from the sample set. As a final check, the connected porosity
425 and P-wave velocity of each sample was measured and any outlying samples were removed
426 from the sample set. This rigorous selection method was employed to minimize the
427 variability within the tested samples, allowing us to compare our data with greater
428 confidence. We note that our measurements are in good agreement with previously
429 published data on NYT quarry samples (e.g., Vanorio et al., 2002; Vinciguerra et al., 2009).
430 We now report that the permeability values presented in this study are not mean values:
431 "Although one sample was used per thermal-stressing temperature, we note that great care
432 was taken during sample selection to exclude samples that contained large heterogeneities
433 and anomalous connected porosities." We have also included information regarding our
434 sample selection procedure:

435
436 "While one of the goals of this contribution is to demonstrate the variability of different tuffs
437 from the CF volcanic district, we strived to minimise the variability between samples cored
438 from the same block by (1) coring many samples and selecting those within a strict porosity
439 range, (2) discarding samples with obvious, large heterogeneities and, (3) discarding
440 samples with anomalous P-wave velocities. Using these sample selection guidelines, our
441 experiments under different conditions (different thermal stressing temperatures and
442 pressures) can be compared with the greatest confidence."

443 3 One more aspect cannot be disregarded: the Authors hypothesize that the investigated samples
444 undergo to mineralogical and physical modifications as a consequence of the increasing
445 temperature and pressure. This can be modeled for outcropping materials but, if one considers the
446 same pyroclastic materials buried for thousands years at different pressure and temperatures, they
447 experienced a mineralogical evolution leading to the formation of an adularia-like feldspar and
448 analcime. It cannot be excluded that the physical and mechanical features of the rocks are
449 significantly different. This minerogenetic process was demonstrated to occur in the zeolitized
450 phlegraean tuffs as described by de Gennaro et al., (2000) for samples of a deep borehole.

451

452 **We agree. In fact, we discuss this at the end of the paper:**

453

454 **“Although our experiments were conducted (1) on samples from the two most widespread
455 tuff lithologies that comprise CF, (2) under the relevant pressures or depths, (3) on water-
456 saturated samples and, (4) over a range of thermal stressing temperatures, our samples
457 were collected from an open quarry and may therefore not represent the material at depth
458 (which have had time to compact, lithify, undergo chemical alteration; e.g., see de Gennaro et
459 al., 2000; see also the report by Giberti et al., 2006). However, we highlight that the
460 permeability measurements on borehole samples presented in the report of Giberti et al.
461 (2006) suggest that (1) the permeability measurements of this study are not dissimilar to
462 those measured on borehole samples and, (2) there is clearly no simple relationship
463 between porosity and permeability...”**

464

465 **We now also offer comparisons between our data and those measured on borehole samples
466 presented in the report of Giberti et al. (2006):**

467

468 **“This conjecture is confirmed by the reduced porosity of samples taken from borehole
469 samples (see the report by Giberti et al., 2006). Measurements on borehole samples from
470 San Vito 1 (at the periphery of the inferred caldera) showed that the porosity decreases from
471 40.5 vol.% at the surface to 32.9, 21.9, 21.9, and 15.1 vol.% at depths of 810, 1420, 2130, and
472 2860 m, respectively. Our data shows that the porosity loss for NYT at 2860 m will be about 9
473 vol.%. A starting porosity of 44 vol.% yields a porosity, purely due to mechanical
474 compaction, of 35 vol.% at a depth of 2860 m. This would imply a porosity loss due to
475 chemical alteration of about 20 vol.% and suggests that the impact of hot, circulating fluids
476 plays the dominant role in the porosity loss of these pyroclastic deposits at depth. Indeed,
477 the report by Giberti et al. (2006) suggests that it is the presence of clay minerals, rather
478 than compaction, that is responsible for the major changes in porosity with depth.**

479

480 **We are certainly aware that our permeability data were collected on rocks from open
481 quarries and, although their properties were measured at the relevant pressures (and under
482 a range of thermal stressing temperatures), may not therefore accurately represent the
483 material at depth (which have had time to compact, lithify, undergo chemical alteration; e.g.,
484 see de Gennaro et al., 2000). However, the open access report of Giberti et al. (2006) offers
485 some permeability data on borehole samples. Data from borehole samples taken from San**

486 **Vito 1 (at the periphery of the inferred caldera) show that, as the porosity is reduced to 32.9,**
487 **21.9, 21.9, and 15.1 vol.% at depths of 810, 1420, 2130, and 2860 m, respectively, the**
488 **permeability (Klinkenberg corrected gas permeabilities) of the samples are 1.1×10^{-13} , $2.5 \times$**
489 **10^{-16} , 7.9×10^{-16} , and 4.9×10^{-16} m², respectively. The permeability of the quarry samples of**
490 **this study are 8.0×10^{-17} m² at a depth of about 2860 m. From these data it is clear that there**
491 **is no simple relationship between the mechanical compaction and chemical alteration that**
492 **afflicted the samples at depth (causing a substantial porosity loss) and their permeability.”**

493

494 4 As far as the paper by Lima et al., the Authors should properly read it as the detailed model of the
495 Campi Flegrei underground and the hypothesis on the causes of bradyseism could strongly
496 invalidate their model.

497

498 **We now discuss the model presented by Lima et al. (2009) in the text:**

499

500 **“The latter category can be broken down further into models that require the input of fresh**
501 **magma from depth (e.g., Gaeta et al., 1998) and those that consider magma body cooling and**
502 **concomitant crystallisation (e.g., Bodnar et al., 2007; Lima et al., 2009).”**

503

504 **However, and we must stress, we are not presenting, or promoting, a model in our paper.**
505 **Our aim was to provide new data to improve the accuracy of the multitude of pre-existing**
506 **models. The model of Lima et al. (2009) still requires knowledge of the elastic properties of**
507 **the rocks within the caldera. They use a Young’s modulus of 9 GPa, a shear modulus of 3 GPa,**
508 **and a Poisson’s ratio of 0.29.**

509

510 5 The Authors refer to Campanian Ignimbrite as a non zeolitized counterpart of NYT. One should
511 remember that a quite large portion of the Campanian Ignimbrite is also zeolitized!

512

513 **This is a good point. We have now included the following sentence: “Although WGI does not**
514 **contain any zeolites, we note that portions of the Campanian Ignimbrite are pervasively**
515 **zeolitized (e.g., see Langella et al., 2013).”**

516

517 6 The Authors report the porosity of zeolitized pyroclastic rocks from Albani Hill, as documented in
518 Vinciguerra et al. I am very doubtful on the fact that a zeolitized material could have such a low
519 porosity. The same rocks usually provide values of 40-45% of porosity.

520

521 **This value of porosity is taken from Vinciguerra et al. (2009). In this paper they state: “In**
522 **contrast to what is commonly observed in outcrops, in the recovered cores the PR displays a**
523 **very well-lithified facies, resulting from a pervasive zeolitization of the ash matrix.” Another**
524 **paper, dealing with the stratigraphy of the Colli Albani from a scientific borehole, also**
525 **reports that the rock is zeolitized: “extremely lithified (zeolitized) ash and scoria deposit”**
526 **(Mariucci et al., 2008). The porosity of this rock was measured using a standard technique**
527 **(helium pycnometry) in Vinciguerra et al. (2009). We therefore have no reason to challenge**
528 **their value.**

529 Mariucci, M. T., Pierdominici, S., Pizzino, L. Marra, F., Montone, P., 2008. Looking into a
530 volcanic area: An overview on the 350 m scientific drilling at Colli Albani (Rome, Italy).
531 *Journal of Volcanology and Geothermal Research*, 176, 225-240.

532
533 The above considerations lead me to consider this paper not suitable for publication.
534

535 **We are confused by the conclusion of “not suitable for publication” by reviewer #3. We feel**
536 **as though we can suitably address all of his comments. Further, we note that this decision is**
537 **a far cry from the positive, and relatively “minor”, revisions suggested by reviewers #1, #2,**
538 **and #4.**

539
540 Line by line comments (on annotated pdf):

541 Page 1084, line 6: According to the quoted authors, the multiphase caldera formed trough at least
542 two high size eruptions, the CI and NYT. Only the latter is phreatoplinian: the former is a purely
543 magmatic ignimbrite forming event.

544
545 **Point taken. This sentence, in response to a comment by reviewer #2, has now been changed**
546 **to respect the hypothesis that the CI could be the result of eruptive events originating from**
547 **pre-existing neotectonic faults. In fact, we removed the word “phreatoplinian”.**

548
549 Page 1084, line 8: Please, quote the right age of ca. 39 ka, reported in De Vivo et al., 2001; DE VIVO,
550 B., ROLANDI, G., GANS, P.B., CALVERT, A., BOHRSON, W.A., SPERA, F.J., BELKIN, H.E., 2001. New
551 constraints on the pyroclastic eruptive history of the Campanian volcanic Plain (Italy). Mineral.
552 Petrol. 73, 47-65. 37 ka, Fedele et al., 2008 FEDELE, L., SCARPATI, C., LANPHERE, M., MELLUSO, L.,
553 MORRA, V., PERROTT,A A., RICCI, G., 2008. The Breccia Museo formation, Campi Flegrei, southern
554 Italy: geochronology, chemostratigraphy and relationship with the Campanian Ignimbrite eruption.
555 Bull. Volcanol. 70, 1189-1219.

556
557 **We agree. We now cite De Vivo et al. (2001): “The eruptive history of the CF volcanic district**
558 **is characterised by two major eruptions: (1) the eruption related to the Campanian**
559 **Ignimbrite about 39,000 years ago (De Vivo et al., 2001) and...”**

560
561 Page 1084, line 9: Please quote the right age of ca 15 ka reported by deino et al. (2004) DEINO, A.L.,
562 ORSI, G., DE VITA, S., PIOCHI, M., 2004. The age of the Neapolitan Yellow Tuff caldera-forming
563 eruption (Campi Flegrei caldera Italy) assessed by 40Ar/39Ar dating method. J. Volcanol. Geotherm.
564 Res. 133, 157-170.

565
566 **We agree. We now cite Deino et al. (2001): “and, (2) the eruption of the Neapolitan Yellow**
567 **Tuff (NYT) about 15,000 years ago (Deino et al., 2004)...”**

568
569 Page 1084, line 11: probably you wanted to write a millennium?
570

571 **Agreed. We have now changed this to: “Although there has not been an eruption for almost**

572 **500 years (since the Monte Nuovo eruption of 1538 AD)..."**

573

574 Page 1084, line 13: In recent times,

575

576 **Agreed: "...In recent times, two major episodes..."**

577

578 Page 1084, line 16: forced to evacuate the

579

580 **We have now changed this sentence: "Surface uplift, on the order of several metres (bradyseism), and accompanying earthquakes in 1984 led to the evacuation of the town of Pozzuoli."**

581

582

583

584 Page 1084, line 19: D'Auria et al. (2011) JGR report the occurrence of an uplift phase starting from

585 2005. The acme of the phase was reached in the September 2012-January 2013 time span. D'Auria

586 L., Giudicepietro F., Aquino I., Borriello G., Del Gaudio C., Lo Bascio D., Martini M., Ricciardi G.P.,

587 Ricciolino P., Ricco C. (2011) - Repeated fluid-transfer episodes as a mechanism for the recent

588 dynamics of Campi Flegrei caldera (1989–2010). Journal of Geophysical Research: Solid Earth, 116.

589

590 **We have now changed this sentence to:**

591

592 **"Since then, there has been an overall subsidence trend (e.g., see Figure 2 in D'Auria et al., 2011), periodically interrupted by small (cm-scale) and short-lived (months) uplifts in 1989, 1994, 2000-2001 (e.g., Lanari et al., 2004; Bianco et al., 2004; D'Auria et al., 2011), and 2004-2006 (e.g., Saccorotti et al., 2007; Trasatti et al., 2008; D'Auria et al., 2011)."**

593

594

595

596

597 Page 1085, line 5: Relies

598

599 **This has now been changed.**

600

601 Page 1086, line 7: a consequence of

602

603 **Agreed. We have now changed this sentence: "...This is usually interpreted as a consequence of the formation of new microcracks..."**

604

605

606 Page 1086, line 9: owing to

607

608 **We would rather keep the wording as it is.**

609

610 Page 1086, line 18: thus confirming what already reported by de Gennaro et al 1983 and 1984 for

611 NYT and zeolitized facies of Campanian Ignimbrite (Industrial Minerals).

612

613 **Yes. But neither of these papers report strength data.**

614

615 Page 1087, line 3: see previous note

616

617 **We have now changed this: “Our experiments were performed on samples of Neapolitan**
618 **Yellow Tuff (NYT) and grey Campanian Ignimbrite (WGI), sampled from the two most**
619 **abundant and widespread volcanic deposits in the CF volcanic district.”**

620

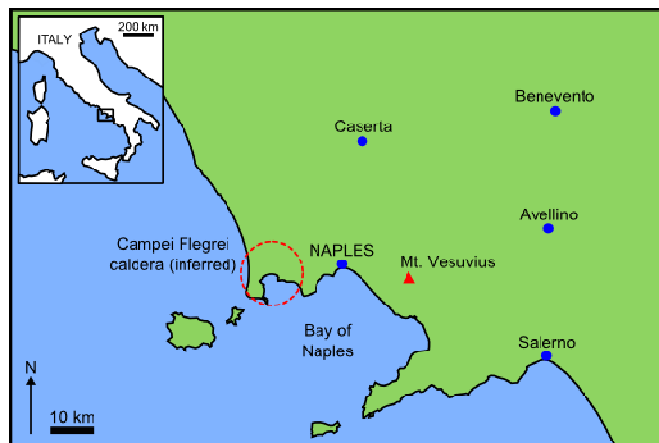
621 Page 1087, line 6: It is necessary to report the sampling area (quarries) localization!

622

623 **We agree. We have now added a new figure (Figure 1 in the revised manuscript, see below)**
624 **showing a map of the Neapolitan region, and new text in the “materials investigated” section:**

625

626 **“NYT was sourced from an open quarry within the inferred CF caldera at Monte San Severino**
627 **(i.e., within the red circle in Figure 1), while the WGI was sourced from an open quarry to the**
628 **north-west of the town of Caserta (the blocks used in this study are the same as those used in**
629 **Heap *et al.*, 2012).**



630

631

632

633

634 **Figure 1. Map showing the location of the inferred Campi Flegrei caldera and the proximity**
635 **of Naples to both the Campi Flegrei caldera and Mt. Vesuvius. The Neapolitan Yellow Tuff**
636 **used in this study was sourced from an open quarry within the inferred CF caldera at Monte**
637 **San Severino (i.e., within the red circle in Figure 1), while the Grey Campanian Ignimbrite**
638 **was sourced from an open quarry to the north-west of the town of Caserta (the blocks used**
639 **in this study are the same as those used in Heap *et al.*, 2012).**

640

641

642 Page 1087, line 7: Display

643

644 **We would prefer to keep “contain”.**

645

646 Page 1087, line 15: Pumiceous

647 Page 1087, line 15: ash mainly made up of glass shards and blocky shaped glass fragments

648 We have now changed this sentence: "...a matrix of **pumiceous** lapilli and **glassy ash (glass**
649 **shards and blocky shaped glass fragments)**..."

650

651 Page 1087, line 22: delete this statement starting from giving

652

653 **Agreed.**

654

655 Page 1087, line 24: LANGELLA, A., BISH, D.L., CAPPELLETTI, P., CERRI, G., COLELLA, A., DE
656 GENNARO, R., GRAZIANO, S.F., PERROTTA, A., SCARPATI, C., DE GENNARO, M., 2013. New insights
657 into the mineralogical facies distribution of Campanian Ignimbrite, a relevant Italian industrial
658 material, *Applied Clay Science* (2013)

659

660 **We have now included this reference in two sentences: "...WGI (Figure 2C and 2D),**
661 **feldspathized by authigenic mineralization processes, is made up of reversely-graded black**
662 **scoriae embedded in an ashy matrix with subordinate lithics and crystals (Cappelletti *et al.*,**
663 **2003; Langella *et al.*, 2013)..." and "...Although WGI does not contain any zeolites, we note**
664 **that portions of the Campanian Ignimbrite are pervasively zeolitized (e.g., see Langella *et al.*,**
665 **2013)..."**

666

667 Page 1088, line 5: Which is the value of ambient humidity?

668

669 **This sentence refers to the laboratory conditions of Zamora *et al.* (1994), Vanorio *et al.***
670 **(2005), and Vinciguerra *et al.* (2006). It is the norm to describe these conditions as "dry".**
671 **However, rock is never completely dry (especially those that contain hydrated minerals!)**
672 **and there is still moisture in the atmosphere. Our aim was to use a term that better respects**
673 **the experimental conditions. We chose "ambient laboratory humidity". However, while we**
674 **note that laboratory humidity is usually quite low, since these studies did not quote**
675 **humidity values, we cannot provide a value.**

676

677 Page 1088, line 8: Specify what kind of fluid phase

678

679 **We have now included this information: "Since the tuffs of CF are present at depth, and are**
680 **likely to contain a fluid phase (e.g., a mixture of meteoric water and seawater contaminated**
681 **by rising magmatic gases, see Valentino *et al.*, 1999), we consider experimental..."**

682

683 Page 1094, line 3: Does the Authors expect a total range of natural variability for samples cored
684 from the same and unique block? I can say it is much wider, on a scale that considers the whole
685 deposit.

686

687 **We agree that the range of natural variability within a 30 cm x 30 cm x 30 cm block of**
688 **material will be much less than the variability of the whole deposit. There is an important**
689 **distinction here. We were keen to measure the physical properties of very different facies in**
690 **order to investigate the variability of the deposits at CF, i.e., we welcomed variability**

691 (although we agree that two facies is unlikely to respect the full extent of the variability,
692 something we discuss at the end of the paper). We chose two rocks that (1) are prevalent in
693 the pre-existing literature, (2) are from the two main eruptions that occurred within the CF
694 volcanic district and, (3) contain different mineral constituents (one with zeolites, and one
695 without). In terms of a “first pass” of the variability at CF, we are unsure we could have
696 chosen better. However, within the individual blocks, we were keen to minimise sample
697 variability. If we want to compare experiments on the same material, but at different
698 conditions (i.e., heated to different temperatures to try to understand the influence of
699 thermal stressing on material properties), the variability between samples must be kept at a
700 minimum so that any differences we see in the data can be attributed to the change in
701 condition, and not the natural variability of the rock. The sentence in question: “The
702 different values obtained for the different thermal stressing temperatures are well within
703 the expected range of natural variability between different samples cored from the same
704 block” refers to the small differences between the curves in the figure. Since these
705 differences are small (in fact, the same scatter would be true for a “well-behaved”
706 sandstone), and show no obvious trend, we can conclude that they are unlikely to be the
707 result of the thermal stressing. We have now included a new paragraph explaining our
708 sample selection procedure:

709
710 **“While one of the goals of this contribution is to demonstrate the variability of different tuffs
711 from the CF volcanic district, we strived to minimise the variability between samples cored
712 from the same block by (1) coring many samples and selecting those within a strict porosity
713 range, (2) discarding samples with obvious, large heterogeneities and, (3) discarding
714 samples with anomalous P-wave velocities. Using these sample selection guidelines, our
715 experiments under different conditions (different thermal stressing temperatures and
716 pressures) can be compared with the greatest confidence.”**

717
718 Page 1096, line 8: I think that the Authors should not disregard how many specimens have been
719 investigated for each test. The sample size is very low, the material is highly heterogeneous. One
720 single data is unacceptable for any kind of consideration. Or the reported data are mean values? In
721 my experience, any new produced data on zeolitized rocks may even more stress the heterogeneity
722 of these rocks.

723
724 **We performed one experiment per condition: our permeability data (a total of 130
725 permeability measurements) do not represent mean values. However, in an attempt to
726 minimise sample variability, all of the samples were cored from the same block and in the
727 same direction. Any anomalous samples (i.e., those containing large crystals, clasts, or
728 pumice lapilli) were removed from the sample set. As a final check, the connected porosity of
729 each sample was measured and any outlying samples were removed from the sample set.
730 This rigorous selection method was employed to minimize the variability within the tested
731 samples, allowing us to compare our data with greater confidence. We now report that the
732 permeability values presented in this study are not mean values: “**Although one sample was
733 used per thermal-stressing temperature, we note that great care was taken during sample****

734 selection to exclude samples that contained large heterogeneities and anomalous connected
735 porosities/P-wave velocities."

736
737 We would certainly expect that any new permeability data would stress the variability of
738 zeolitized rocks (although, any new data would also be measured on "small" samples). We
739 would welcome these data; in fact, one of the conclusions of our paper is that more
740 experiments on the full range of materials are now needed to assess the extent of the
741 variability at Campi Flegrei.

742
743 Page 1096, line 14: Not surprising at all! The problem is not the slight difference in porosity. If you
744 consider the specific surface area of the two materials there is an order of magnitude difference. A
745 zeolitized tuff with about 50% of zeolite has a 8-9% of water (wt.%) content at ambient
746 temperature vs 0% for WGI.

747
748 While we are inclined to agree that the specific surface area of these materials are probably
749 quite different, the link between permeability and specific surface area is not as simple as
750 depicted by reviewer #3. For example, Bentheim sandstone, which has a porosity of 23 vol.%
751 and a permeability of about $1.0 \times 10^{-12} \text{ m}^2$ has the same specific surface area as Lanhein
752 granite, which has a porosity of about 1 vol.% and a permeability of about $1.0 \times 10^{-19} \text{ m}^2$. We
753 suspect that the difference in permeability is more related to the difference in
754 microstructure (i.e., the connectivity of the porosity). We have changed the text to emphasise
755 our stance on this matter:

756
757 "This difference in permeability could be considered surprising if one were to solely
758 consider their connected porosities (44 and 49 vol.% for NYT and WGI, respectively). The
759 difference in permeability is likely due to differences in pore space connectivity, perhaps
760 related to the extent of zeolitization and lithification. A similar conclusion was drawn by
761 Vinciguerra *et al.* (2009)."

762
763 Page 1096, line 20: I made a lot of porosity measurements on the zeolitized tuff from Albani Hill and
764 I never found such a low porosity value.

765
766 This value of porosity is taken from Vinciguerra *et al.* (2009). In this paper they state: "In
767 contrast to what is commonly observed in outcrops, in the recovered cores the PR displays a
768 very well-lithified facies, resulting from a pervasive zeolitization of the ash matrix." Another
769 paper, dealing with the stratigraphy of the Colli Albani from a scientific borehole, also
770 reports that the rock is zeolitized: "extremely lithified (zeolitized) ash and scoria deposit"
771 (Mariucci *et al.*, 2008). The porosity of this rock was measured using a standard technique
772 (helium pycnometry) in Vinciguerra *et al.* (2009). We therefore have no reason to challenge
773 their value.

774

775 Mariucci, M. T., Pierdominici, S., Pizzino, L. Marra, F., Montone, P., 2008. Looking into a
776 volcanic area: An overview on the 350 m scientific drilling at Colli Albani (Rome, Italy).
777 *Journal of Volcanology and Geothermal Research*, 176, 225-240.

778
779 Page 1097, line 19: They are NYT and WGI only from a volcanological point of view. From a
780 mineralogical and petrophysical point of they are something else.

781
782 **This is a rather cryptic comment. NYT is not NYT from a mineralogical or petrophysical point**
783 **of view?**

784
785 Page 1098, line 3: That is exactly the percent of water bound to zeolites and smectites always
786 occurring in NYT! You can easily achieve this value by a simple LOI

787
788 Yes. The reported number, from Heap et al. (2012), was determined by simple loss-on-
789 ignition (thermo-gravimetric) analysis. The NYT used in this study is from the same blocks
790 used in Heap et al. (2012). We have now reworded this sentence to make this more explicit:
791 "[Heap et al. \(2012\) showed, using a combination of](#) thermo-gravimetric analysis, optical
792 microscopy, and X-ray diffraction, that NYT lost 18% of its initial mass..."

793
794 Page 1098, line 15: Wrong citation. The paper is de Gennaro et al., 1987.

795
796 **De Gennaro and Colella (1989) summarise the findings of the key papers on the influence of**
797 **temperature on hydrated tuff from Campi Flegrei. We would prefer to keep this reference**
798 **(that also cites de Gennaro et al., 1987). However, we are aware that not all of the data in de**
799 **Gennaro and Colella (1989) are unique to this study. We have now changed this sentence to:**
800 **"Phillipsite breaks down during dehydration and chabazite undergoes reversible hydration**
801 **at 350 °C, and, by 900 °C, the structure of the zeolites will be so damaged that no further**
802 **water molecules can be stored (see de Gennaro and Colella, 1989 and references therein)."**

803
804 Page 1098, line 17: These two phenomena are strongly interconnected as the framework collapse of
805 zeolites defines a shrinkage of the specimen and the consequent cracks.

806
807 **Agreed. We have now altered the wording of this sentence: "Therefore, the reported changes**
808 **in NYT physical properties are due to a combination of thermal cracking and the cracks**
809 **formed as a result of the disintegration of the material through the loss of zeolites."**

810
811 Page 1102, line 6:that whoever studies NYT and Campanian Ignimbrite well knows.....

812
813 **Yes. But we show, for the first time, the heterogeneity in permeability and elastic moduli of**
814 **different tuffs from Campi Flegrei.**

815
816 A e B sono ad ingrandimenti diversi e quindi non confrontabili. Ovviamente anche in questo caso
817 vale la considerazione sulla eterogeneità del materiale.

818 All of the SEM pictures in Figure 10 (now Figure 11) were taken under different
819 magnifications. Our aim with panel A was to show an overview of the post-P* microstructure,
820 whilst panels B and C focus on evidence for pore collapse. It was never our intention to
821 compare panels A and B. However, we appreciate that we do not clearly explain this in either
822 the text or the figure caption. We have now changed the figure caption to:
823

824 "Figure 11. Scanning electron microscope images of an as-collected sample of Neapolitan
825 Yellow Tuff taken beyond P*. Panel A shows an overview of the post-P* microstructure at a
826 low magnification. Panels B and C show detailed evidence of pore collapse (indicated by the
827 white arrows). Panel C is a zoom of the white box shown in panel B."
828

829 Reviewer #4 (anonymous)

830

831 The paper "The permeability and elastic moduli of tuff from Campi Flegrei, Italy: implications for
832 ground deformation modelling" concerns estimation of parameters which are critical in the
833 evaluation of the Campi Flegrei caldera deformation due to injection of both magma or magmatic
834 fluids. The argument is of great interest, as acquisition of data on deformation of the caldera is in
835 progress as number and quality, and it would deserves the publication.

836

837 **We are pleased that reviewer #4 deems our work "critical", "of great interest", and that it**
838 **"deserves the publication".**

839

840 Some critical question arise:

841

842 1) the samples used by author, if I understood, seams (line 7, section material investigated) relative
843 to one block of material for type (NYT and WGI) and collected in open quarries, and the estimated
844 porosity is 44 and 49 vol.% respectively. The Phlegrean Field show a very high variability in
845 porosity and permeability (see for examples http://www.fedoa.unina.it/398/1/Campi_Flegrei.pdf
846 where core samples by AGIP oil company are analyzed) even at the same sampling depth (different
847 wells) showing that not only temperature and pressure act on these parameters but evidently these
848 depend on lithotypes and alteration degree; moreover if we consider even the dependence on
849 depth, values of porosity range from some % to about 60% while permeability change up to 3
850 magnitude order and more. This mean, in general, extrapolation of the analysis performed in the
851 paper are difficult to sustain and extend to the whole caldera sediments, and it as it stand seems
852 applicable only to that open quarry samples.

853

854 **We agree that the rocks of Campi Flegrei span a wide range of porosity and permeability. For**
855 **example, in the report (which is not peer reviewed) highlighted by the reviewer, the**
856 **porosity of the rocks in the San Vito 1 well are 40.5% near the surface and 15.1% at a depth**
857 **of 2860 m. Low porosity (6-8%) lavas were encountered in some of the other wells. The**
858 **permeability of the aforementioned borehole tuff samples ranges from 10^{-13} to 10^{-16} m². The**
859 **permeabilities of our open quarry samples also span a similar range (from 10^{-13} to 10^{-15} m²**
860 **at $P_{eff} = 5$ MPa). While we understand that our samples may not accurately represent the**
861 **rock at depth (due to compaction, lithification, alteration), we would contend that (1)**
862 **measurements on tuffs from Campi Flegrei are actually extremely rare, adding interest to**
863 **our open quarry rock data (further, we feel that we are very open about the limitations of**
864 **our data), (2) that our data still highlight that the physical properties of the tuffs of Campi**
865 **Flegrei can be very variable. We agree that, using our data, it is difficult to "extend to the**
866 **whole caldera sediments", but, and as we conclude in the paper, we envisage that our data**
867 **simply highlight that consideration should be afforded to the input parameters in ground**
868 **deformation modelling and the need for more experimental studies, using our study as a**
869 **stepping stone. We have now added several paragraphs discussing the difference between**
870 **our data and data from borehole samples:**

871

872 "This conjecture is confirmed by the reduced porosity of samples taken from borehole
873 samples (see the report by Giberti *et al.*, 2006). Measurements on borehole samples from
874 San Vito 1 (at the periphery of the inferred caldera) showed that the porosity decreases from
875 40.5 vol.% at the surface to 32.9, 21.9, 21.9, and 15.1 vol.% at depths of 810, 1420, 2130, and
876 2860 m, respectively. Our data shows that the porosity loss for NYT at 2860 m will be about 9
877 vol.%. A starting porosity of 44 vol.% yields a porosity, purely due to mechanical
878 compaction, of 35 vol.% at a depth of 2860 m. This would imply a porosity loss due to
879 chemical alteration of about 20 vol.% and suggests that the impact of hot, circulating fluids
880 plays the dominant role in the porosity loss of these pyroclastic deposits at depth. Indeed,
881 the report by Giberti *et al.* (2006) suggests that it is the presence of clay minerals, rather
882 than compaction, that is responsible for the major changes in porosity with depth.
883

884 We are certainly aware that our permeability data were collected on rocks from open
885 quarries and, although their properties were measured at the relevant pressures (and under
886 a range of thermal stressing temperatures), may not therefore accurately represent the
887 material at depth (which have had time to compact, lithify, undergo chemical alteration; e.g.,
888 see de Gennaro *et al.*, 2000). However, the open access report of Giberti *et al.* (2006) offers
889 some permeability data on borehole samples. Data from borehole samples taken from San
890 Vito 1 (at the periphery of the inferred caldera) show that, as the porosity is reduced to 32.9,
891 21.9, 21.9, and 15.1 vol.% at depths of 810, 1420, 2130, and 2860 m, respectively, the
892 permeability (Klinkenberg corrected gas permeabilities) of the samples are 1.1×10^{-13} , $2.5 \times$
893 10^{-16} , 7.9×10^{-16} , and 4.9×10^{-16} m², respectively. The permeability of the quarry samples of
894 this study are 8.0×10^{-17} m² at a depth of about 2860 m. From these data it is clear that there
895 is no simple relationship between the mechanical compaction and chemical alteration that
896 afflicted the samples at depth (causing a substantial porosity loss) and their permeability."
897

898 2) A second question arise relative to the usefulness of the relation found by authors about
899 permeability and porosity and showed in the figure 3 and 4. The sample analyzed by authors has
900 been subject to a different history from the NYT and WGI sediments which fill the caldera at
901 different depth and different time; pressure, time and temperature contribute heavily to the
902 alteration of the materials. It should be performed analysis, by the authors, to some sample
903 collected at different depths to contribute in a substantial improving of our knowledge on the
904 caldera. Papers relative to the physical parameters of the caldera use widely measurements on
905 cored samples. These are, for example, analysis of permeability and porosity on cored samples for
906 which suddenly decrease both pressure and temperature as they are extracted from the wells. The
907 question touched by the authors is critical and it would be very interesting if they could measure
908 hysteresis curves; the curves in fig 4 beyond the P* point clearly shows irreversible processes, as
909 stated in the paper. If authors could show some curves with hysteresis cycles it could contribute to
910 the extrapolation of the measured parameters to the original state before the extraction of the
911 sample from the wells.
912

913 We agree that the history of our samples (heating them to different temperatures and
914 pressurising them in a pressure vessel) differs from the natural case. We discuss this at

length in the discussion section (and we have included new discussion, see our answers above). In fact, we conclude by stating that measurements on borehole samples are more representative and that future studies should focus in this direction. However, and we would still argue the case, there are extremely few papers that contain such data. The report "Geophysical Exploration of the Campi Flegrei (Southern Italy) Caldera' Interiors: Data, Methods and Results" highlighted by the reviewer certainly contains some interesting data, but this document was not peer-reviewed. For instance, there is extremely little information on how the permeability values were measured (confining pressure? pore fluid pressure? pressure gradient?...). Unfortunately, we did not measure permeability while we were reducing the confining pressure on the sample. We do understand the interest of this. However, in the scenario described by the reviewer, perhaps this is best done on samples taken from boreholes.

3) page 1092 row 1-5. Authors stated that they estimate the values of the young modulus in the linear zone at effective pressure of 5 Mbar, but in order to render usefulness the static modules, to apply static elasticity modelisation at episodes of deformation, they would estimate the static moduli at different pressure and temperature or show that they do not depend on these variables or in negligible way.

Our goal was to simply demonstrate the difference between static and dynamic moduli under the same pressure conditions. We completely agree that the static (and dynamic, see Figures 7 and 8) moduli will change with increasing pressure or temperature. Rock will be stiffer at higher pressures. For example, we measured the Young's modulus for an unpublished "wet" uniaxial experiment on NYT and found a value of 1.6 GPa (lower than the 2.1 GPa found at 5 MPa). However, our high porosity quarry samples are already ductile at 5 MPa: at higher pressures the "elastic window" may well be negligible. Further, P^* is at about 15 MPa. To satisfy the reviewer's request, static elastic moduli should be measured on borehole samples (that contain a lower porosity). However, no such data exists (and we do not have borehole samples). We have now added a sentence to this effect in the paper:

"We note that, while values of the shear modulus of borehole samples provided in the report of Giberti et al. (2006) show that the dynamic shear modulus can reach values of 10.9 GPa at a depth of 2860 m, no complementary static values exist. Future research should focus on the determination of the static elastic moduli of borehole samples."

Minor comments

In all the relations showed in figures and in tables it lack the error bars, making it difficult to evaluate the graphs.

In fact, the error bars are very small. The natural sample variability – something we tried to minimise – is much larger. We now include tables showing the expected measurement

957 **accuracies and sample variability, and discussion on our method to reduce the variability**
958 **between samples cored from the same block (see our answers above).**

959

960 page 1101 row 11-12. I would not say that data analyzed emphasized the heterogeneous nature of
961 the tuffs of the caldera, they are only 2 types of tuffs

962 page 1102 row 5-6. Hold the same comment as the previous.

963

964 **Perhaps our data do not respect the full extent of the variability. But, our tuffs still display a**
965 **difference in permeability of two orders of magnitude. We have now expanded the sentence**
966 **in our conclusions to emphasise the fact that we do not capture the full extent of the**
967 **variability at CF:**

968

969 **“While we urge that these new laboratory data should be considered in routine ground**
970 **deformation modelling, our study highlights that the physical properties of just two rocks**
971 **that comprise the caldera at Campi Flegrei can be extremely heterogeneous (we also**
972 **anticipate that future measurements will further expand our knowledge of such**
973 **heterogeneity).”**

974

975 page 1117 figure 5 B. There is a strange intersection of the permeability/pressure curves at
976 different temperature around 12-30 MPa, it deserve probably some explanation, or error bars could
977 include it?

978

979 **We discuss this in the text. It is due to the natural variability between samples cored from**
980 **the same block (not measurement error). However, we did our best to avoid variability**
981 **between samples cored from the same block, and we now provide our transducer accuracies**
982 **and the expected natural variability as Tables 2 and 3 (see our answers above).**

983 The permeability and elastic moduli of tuff from Campi Flegrei, Italy:
984 Implications for ground deformation modelling

985

986 M. J. Heap¹, P. Baud¹, P. G. Meredith², S. Vinciguerra^{3,4}, and T. Reuschlé¹

987

988 ¹*Laboratoire de Déformation des Roches, Équipe de Géophysique Expérimentale, Institut de
989 Physique de Globe de Strasbourg (UMR 7516 CNRS, Université de Strasbourg/EOST), 5 rue
990 René Descartes, 67084 Strasbourg cedex, France.*

991 ²*Rock & Ice Physics Laboratory, Department of Earth Sciences, University College London,
992 Gower Street, London WC1E 6BT, UK.*

993 ³*Department of Geology, University of Leicester, University Road, Leicester, LE1 7RH, UK.*

994 ⁴*British Geological Survey, Environmental Science Centre, Keyworth, Nottingham, NG12 5GG,
995 UK.*

996

997 **Abstract**

998

999 The accuracy of ground deformation modelling at active volcanoes is a principal requirement in
1000 volcanic hazard mitigation. However, the reliability of such models relies on the accuracy of the
1001 rock physical property (permeability and elastic moduli) input parameters. Unfortunately,
1002 laboratory-derived values on representative rocks are usually rare. To this end we have
1003 performed a systematic laboratory study [on](#) the influence of pressure and temperature on the
1004 permeability and elastic moduli of [samples from](#) the two most widespread [lithified pyroclastic](#)

1005 deposits at the Campi Flegrei volcanic district, Italy. Our data show that the water permeability
1006 of Neapolitan Yellow Tuff and a tuff from the Campanian Ignimbrite differ by about 1.5 orders
1007 of magnitude. As pressure (depth) increases beyond the critical point for inelastic pore collapse
1008 (at an effective pressure of 10-15 MPa, or a depth of about 750 m), permeability and porosity
1009 decrease significantly, and ultrasonic wave velocities and dynamic elastic moduli increase
1010 significantly. Increasing the thermal stressing temperature increases the permeability and
1011 decreases the ultrasonic wave velocities and dynamic elastic moduli of the Neapolitan Yellow
1012 Tuff; whereas the tuff from the Campanian Ignimbrite remains unaffected. This difference is due
1013 to the presence of thermally unstable zeolites within the Neapolitan Yellow Tuff. For both rocks
1014 we also find, under the same pressure conditions, that the dynamic (calculated from ultrasonic
1015 wave velocities) and static (calculated from triaxial stress-strain data) elastic moduli differ
1016 significantly. The choice of elastic moduli in ground deformation modelling is therefore an
1017 important consideration. While we urge that these new laboratory data should be considered in
1018 routine ground deformation modelling, we highlight the challenges for ground deformation
1019 modelling based on the heterogeneous nature (vertically and laterally) of the rocks that comprise
1020 the caldera at Campi Flegrei.

1021

1022 **1. Introduction**

1023

1024 Monitoring ground deformation, the surface expression of deeper magmatic and/or hydrothermal
1025 activity, at active volcanoes is an important tool in volcanic hazard forecasting and mitigation.
1026 Ground deformation at a volcano [measured by global positioning system (GPS) satellites,
1027 interferometric synthetic aperture radar (InSAR), tiltmeters, or electronic distance metres

1028 (EDM)] are typically analysed using inverse problem models that consider a source (e.g., a
1029 magma chamber, a zone of overpressurised fluids, or a combination of the two) embedded within
1030 a homogenous elastic or viscoelastic half-space (e.g., Mogi, 1958; Dzurisin, 2006; Hurwitz *et al.*,
1031 2007). These models yield important information regarding the location, shape, and
1032 volume/pressure changes of the source. The accuracy of such modelling relies on the accuracy of
1033 the rock physical property input parameters (typically elastic moduli and permeability,
1034 depending on the type of model). Even small changes in the values of key controlling parameters
1035 can lead to large differences in the rate, magnitude, and geometry of ground surface deformation
1036 (e.g., Hurwitz *et al.*, 2007). For instance, a recent contribution using viscoelastic modelling to
1037 better understand flank motion and summit subsidence at Kīlauea (Hawai'i) showed that
1038 deformation rates are enhanced when the elastic moduli input parameters are lowered (Plattner *et*
1039 *al.*, 2013). Furthermore, homogenous half-space models, by definition, assume that [all](#) the rocks
1040 that comprise the volcano have identical physical properties. However, volcanoes are built from
1041 successive eruptive episodes and thus the physical properties of the rock strata that form the
1042 edifice are likely to span a wide range. For this reason, conventional homogenous half-space
1043 modelling at volcanoes has recently been considered an oversimplification that could lead to
1044 misinterpretation of the derived source parameters (Manconi *et al.*, 2007; Manconi *et al.*, 2010).
1045 For instance, Manconi *et al.* (2010) showed that this “standard” approach can lead to inaccurate
1046 values for the source volume changes. Therefore, models that consider mechanical
1047 heterogeneities (e.g., Manconi *et al.*, 2007; Manconi *et al.*, 2010) require a good knowledge of
1048 the breadth of elastic moduli that can be expected for representative rocks, and [thermodynamic](#)
1049 [and magmatic-hydrothermal](#) models (e.g., Hurwitz *et al.*, 2007; Todesco *et al.*, 2010) require

1050 accurate values of their permeability and elastic moduli. However, such laboratory data are
1051 commonly scarce or absent.

1052

1053 The densely populated (about 3 million) Neapolitan area, southern Italy, is in a state of constant
1054 threat provided by the proximity of Mt. Vesuvius and the increasingly-restless Campi Flegrei
1055 (CF) volcanic district (Ricci *et al.*, 2013; Figure 1). The eruptive history of the CF volcanic
1056 district can be characterised by two major eruptions: (1) the eruption related to the emplacement
1057 of the Campanian Ignimbrite about 39,000 years ago (De Vivo *et al.*, 2001) and, (2) the eruption
1058 of the Neapolitan Yellow Tuff (NYT) about 15,000 years ago (Deino *et al.*, 2004); although the
1059 area has been volcanically active for more than 300,000 years (Rolandi *et al.*, 2003).

1060

1061 Today, the CF volcanic district is dominated by a resurgent, nested caldera (Figure 1) that hosts a
1062 large, shallow (< 4 km) hydrothermal system (e.g., De Natale *et al.*, 2006). The CF caldera is
1063 considered to have formed due to collapse following (1) both of the major eruptions (e.g.,
1064 Barberi *et al.*, 1991; Orsi *et al.*, 1996) or, (2) the eruption of the NYT only (see Rolandi *et al.*,
1065 2003 and references therein). In the latter hypothesis, the Campanian Ignimbrite is thought to be
1066 the result of eruptive events originating from pre-existing neotectonic faults formed during the
1067 Apennine uplift (De Vivo *et al.*, 2001; Rolandi *et al.*, 2003). Although there has not been an
1068 eruption for almost 500 years (since the Monte Nuovo eruption of 1538 AD), CF has become
1069 increasingly restless and is densely monitored by permanent seismic and ground deformation
1070 networks. In recent times, two major episodes of unrest have occurred, between 1969-1972 and
1071 1982-1984 (Bianchi *et al.*, 1987; Bonafede, 1991). Surface uplift, on the order of several metres
1072 (bradyseism), and accompanying earthquakes in 1984 led to the evacuation of the town of

1073 Pozzuoli. Since then, there has been an overall subsidence trend (e.g., see Figure 2 in D'Auria *et*
1074 *al.*, 2011), periodically interrupted by small (cm-scale) and short-lived (months) uplifts in 1989,
1075 1994, 2000-2001 (e.g., Lanari *et al.*, 2004; Bianco *et al.*, 2004; D'Auria *et al.*, 2011), and 2004-
1076 2006 (e.g., Saccorotti *et al.*, 2007; Trasatti *et al.*, 2008; D'Auria *et al.*, 2011). However, the
1077 interpretation of long-term and short-term ground deformation patterns at CF is a matter of
1078 debate (see De Natale *et al.*, 2001 and De Natale *et al.*, 2006 for reviews on the topic). Models to
1079 explain the origin of the uplift can be broadly divided into two camps: those that consider solely
1080 the input of magma at depth (e.g., Berrino *et al.*, 1984; Bonafede *et al.*, 1986; Bianchi *et al.*,
1081 1987) and those that invoke an interaction between magma and fluids (magmatic-hydrothermal
1082 models and thermodynamic models; e.g., Bonafede, 1991; Gaeta *et al.*, 1998; Bonafede and
1083 Mazzanti, 1998; De Natale *et al.*, 2001; Lundgren *et al.*, 2001; Troise *et al.*, 2001; Gaeta *et al.*,
1084 2003; Chiodini *et al.*, 2003; Battaglia *et al.*, 2006; Gottsmann *et al.*, 2006; Troise *et al.*, 2007;
1085 Bodnar *et al.*, 2007; Lima *et al.*, 2009; Todesco *et al.*, 2010; D'Auria *et al.*, 2011; Troiano *et al.*,
1086 2011; Chiodini *et al.*, 2012). The latter category can be broken down further into models that
1087 require the input of fresh magma from depth (e.g., Gaeta *et al.*, 1998) and those that consider
1088 magma body cooling and concomitant crystallisation (e.g., Bodnar *et al.*, 2007; Lima *et al.*,
1089 2009). Other models account for the surface deformation by invoking an interaction between the
1090 pressure source and caldera boundary fractures (e.g., De Natale and Pingue, 1993; Beauducel *et*
1091 *al.*, 2004) or mechanical heterogeneities (e.g., Manconi *et al.*, 2010).

1092

1093 While we note that the goal of this contribution is not to critically review the numerous models
1094 invoked to explain the ground deformation at CF, we highlight that the accuracy of all these
1095 models relies on accuracy of the rock physical property input parameters. Unfortunately,

1096 published laboratory investigations on the physical properties of representative materials from
1097 the CF caldera are rare. Values of permeability have, thus far, either been inferred from *in-situ*
1098 observations (Rosi and Sbrana, 1987) or have been taken from experiments conducted on NYT
1099 under ambient pressure conditions (Ascolese *et al.*, 1993a; Ascolese *et al.*, 1993b; Peluso and
1100 Arienzo, 2007). In the most recent study, Peluso and Arienzo (2007) measured the permeability
1101 of NYT at ambient pressure to be between 2.0×10^{-15} and 6.3×10^{-17} m² (the range of porosity
1102 was between 48 and 52 vol.%). However, not only are the deposits within the CF caldera present
1103 at depth (which is likely to severely influence their permeability), but it is known that the
1104 permeability of lithified pyroclastic deposits can be highly variable (a variety of representative
1105 materials should therefore be measured), depending on their degree of lithification (Vinciguerra
1106 *et al.*, 2009). We also highlight that permeability data of borehole samples are presented in an
1107 open access report (Giberti *et al.*, 2006). For example, this report shows, for the San Vito 1
1108 borehole, that the permeability can range from 10^{-13} m² at the surface to 10^{-16} m² at a depth of
1109 almost 3000 m.

1110

1111 Elastic moduli are generally assumed, or extrapolated from seismic tomography studies (e.g.,
1112 Chiarabba and Moretti, 2006; Vinciguerra *et al.*, 2006). Typically, Poisson's ratio is taken as 0.3
1113 and shear modulus as 5 GPa (e.g., De Natale *et al.*, 1991). However, dynamically-determined
1114 elastic moduli (i.e., those calculated from ultrasonic wave velocities) may not represent the most
1115 appropriate values to use in volcano ground deformation modelling. Deformation caused by a
1116 volcanic source proceeds quasi-statically rather than dynamically and therefore static elastic
1117 moduli are likely to be the most appropriate input parameters (Heap *et al.*, 2009; Manconi *et al.*,
1118 2010). It is well known that dynamic and static moduli differ as a result of the large differences

1119 in the frequency at which they were measured (Simmons and Brace, 1965; Cheng and Johnston,
1120 1981; Eissa and Kazi, 1989; Ciccotti and Mulargia, 2004; Ciccotti *et al.*, 2004). Static elastic
1121 moduli for representative materials from CF are not yet available (see Manconi *et al.*, 2010).

1122
1123 The pyroclastic deposits that comprise the caldera at CF are exposed to elevated temperatures, as
1124 evidenced by two-dimensional conductive/convective numerical modelling (Wohletz *et al.*,
1125 1999), seismic attenuation tomography (de Lorenzo *et al.*, 2001), and infrared imaging (Chiodini
1126 *et al.*, 2007). Surface geothermal gradients of about 150-200 °C/km are estimated (for the first
1127 1.5 km) and, at the edge of the hydrothermal system, a temperature of 420 °C was measured at a
1128 depth of 3 km (AGIP borehole San Vito 1, de Lorenzo *et al.*, 2001). It has been shown
1129 previously that thermal stresses can increase the permeability (e.g., Homand-Etienne and
1130 Troalen, 1984; Jones *et al.*, 1997; David *et al.*, 1999; Nara *et al.*, 2011) and decrease the Young's
1131 modulus (e.g., Keshavarz *et al.*, 2010) of rock. This is usually interpreted as being a consequence
1132 of the formation of new microcracks due to the build-up of internal thermal stresses. Volcanic
1133 rocks are persistently challenged by elevated temperatures due to their proximity to large
1134 permanent heat sources, and the fluctuations in temperature caused by the movement of magma,
1135 are therefore especially prone to thermal microcracking. Furthermore, many fine-grained
1136 pyroclastic deposits can be further jeopardised by thermal stresses due to the presence of
1137 thermally unstable zeolites (Heap *et al.*, 2012). Since zeolitization promoted lithification, the loss
1138 of zeolites can impose dramatic consequences on rock physical properties. Recent data has
1139 shown that NYT becomes structurally unstable upon exposure to high (100-750 °C)
1140 temperatures, resulting in a severe decrease in both tensile and compressive strength (Heap *et al.*,
1141 2012). A recent contribution by Manconi *et al.* (2010) highlighted the need for the evaluation of
1142 the temperature-dependence of the material properties of the rocks at CF.

1143

1144 For the reasons outlined above we **have conducted** a systematic study of the influence of pressure
1145 and temperature on the physical properties (permeability, porosity, ultrasonic velocities, and
1146 elastic moduli) of two **lithified pyroclastic deposits** (one zeolitized) from CF. We first present the
1147 investigated materials and methods. We then present our experimental results before discussing
1148 our data in terms of **ground deformation** modelling at CF.

1149

1150 **2. Materials investigated**

1151

1152 Our experiments were performed on samples of Neapolitan Yellow Tuff (NYT) and grey
1153 Campanian Ignimbrite (WGI), sampled from the two most abundant and widespread volcanic
1154 deposits in the CF volcanic district. NYT was sourced from an open quarry within the inferred
1155 CF caldera at Monte San Severino (i.e., within the red circle in Figure 1), while the WGI was
1156 sourced from an open quarry to the north-west of the town of Caserta (the blocks used in this
1157 study are the same as those used in Heap *et al.*, 2012). In this paper we refer to both lithified
1158 pyroclastic rocks as “tuffs”.

1159

1160 NYT and WGI contain average connected porosities of 44 and 49 vol.%, respectively (measured
1161 using the triple weight water saturation technique; Guéguen and Palciauskas, 1994). **We note**
1162 **that, although our samples are small compared to the volume of the natural deposits, a report by**
1163 **Giberti *et al.* (2006) showed that the porosity of 12 cm³ and 125 cm³ samples were very similar,**
1164 **for a wide range of material from CF.** Photographs and optical microscopy photomicrographs of
1165 the samples are provided as Figure 2 and their ambient pressure, “as-collected” (i.e., “natural”

1166 samples that have undergone no heating or deformation) physical properties are listed in Table 1.
1167 NYT (Figure 2A and 2B), a trachytic pyroclastic deposit characterized by both pyrogenic and
1168 authigenic phases (de Gennaro *et al.*, 2000), contains phenocrysts of sanidine, plagioclase,
1169 clinopyroxene, biotite, and minor amounts of Ti-magnetite and apatite within a matrix of
1170 **pumiceous** lapilli and **glassy ash (glass shards and blocky shaped glass fragments)**. X-ray
1171 diffraction pattern analysis has indicated the presence of phillipsite, chabazite, and analcime
1172 (Heap *et al.*, 2012). The mean content of these zeolites in NYT can exceed 50 wt. % (e.g., de
1173 Gennaro *et al.*, 1990; de Gennaro *et al.*, 2000). WGI (Figure 1C and 1D), feldspathized by
1174 authigenic mineralization processes, is made up of reversely-graded black scoriae embedded in
1175 an ashy matrix with subordinate lithics and crystals (Cappelletti *et al.*, 2003; Langella *et al.*,
1176 2013). WGI contains hypidiomorphic phenocrysts of alkali-feldspars with minor amounts of
1177 clinopyroxene, as well as microlites of alkali-feldspar, Ti-magnetite and apatite. The matrix
1178 comprises well-sorted glass shards with occasional accretionary ash clots and porous lapilli
1179 fragments (Heap *et al.*, 2012 and references therein). Although WGI does not contain any
1180 **zeolites**, we note that portions of the Campanian Ignimbrite are pervasively zeolitized (e.g., see
1181 Langella *et al.*, 2013).

1182

1183 **3. Experimental methods**

1184

1185 The caldera at CF hosts a large, shallow (< 4 km) hydrothermal system (e.g., De Natale *et al.*,
1186 2006). Indeed, laboratory studies have demonstrated that water-saturated ultrasonic velocities on
1187 tuffs from CF are more representative of the *in-situ* values than “dry” (measurements conducted
1188 on oven dried samples at ambient laboratory humidity) ultrasonic velocities (Zamora *et al.*, 1994;

1189 Vanorio *et al.*, 2005; Vinciguerra *et al.*, 2006). Since the tuffs of CF are present at depth, and are
1190 likely to contain a fluid phase (e.g., a mixture of meteoric water and seawater contaminated by
1191 rising magmatic gases, see Valentino *et al.*, 1999), we consider experimental values on
1192 pressurised, water-saturated samples as the most representative. Our experimental program was
1193 twofold. (1) Hydrostatic (i.e., $\sigma_1 = \sigma_2 = \sigma_3$) experiments to measure changes in permeability,
1194 porosity, ultrasonic wave velocities, and dynamic elastic moduli with increasing effective
1195 pressure (Peff, from 5 MPa to 50 MPa) on samples that had been thermally stressed to a range of
1196 temperatures (from as-collected to 1000 °C). (2) Constant strain rate conventional triaxial (i.e.,
1197 $\sigma_1 > \sigma_2 = \sigma_3$) deformation experiments at a Peff of 5 MPa to measure static elastic moduli.
1198 Importantly, we measure both static and dynamic elastic moduli at the same Peff (= 5 MPa) so
1199 that the values can be easily compared. All our experiments were performed at room temperature
1200 (while this may not accurately represent the natural case, we note that, to explore the influence of
1201 temperature on the physical properties of the tuffs, we conducted experiments on samples
1202 thermally stressed to a range of temperatures).

1203

1204 Experimental data are subject to error as a result of the accuracy of the various transducers.
1205 Estimations of the accuracy of the measurements of this study are listed in Table 2. The errors
1206 are extremely small and lead to error bars that are smaller than the data points in the figures
1207 provided in this study. However, we note that measurement errors are dwarfed by the natural
1208 sample variability of the tuffs (i.e., the natural variability of samples cored from the same block
1209 of material). Estimations of the natural sample variability of the tuffs used this study are
1210 provided in Table 3. While one of the goals of this contribution is to demonstrate the variability
1211 of different tuffs from the CF volcanic district, we strived to minimise the variability between

1212 samples cored from the same block by (1) coring many samples and selecting those within a
1213 strict porosity range, (2) discarding samples with obvious, large heterogeneities and, (3)
1214 discarding samples with anomalous P-wave velocities. Using these sample selection guidelines,
1215 our experiments under different conditions (different thermal stressing temperatures and
1216 pressures) can be compared with the greatest confidence.

1217

1218 3.1 Hydrostatic experiments

1219

1220 Hydrostatic experiments were performed in the Rock & Ice Physics Laboratory (RIPL) at
1221 University College London (UCL) using a 300 MPa hydrostatic pressure vessel equipped with
1222 two 70 MPa servo-controlled pore fluid intensifiers or volumometers (Figure 3, see also
1223 Kolzenburg *et al.*, 2012). The apparatus is designed to measure permeability, porosity, and
1224 ultrasonic wave velocities contemporaneously. In our experiments we chose an experimental
1225 pressure range of 5-50 MPa (i.e., up to a depth of about 3.5 km).

1226

1227 Cylindrical samples, 25 mm in diameter and nominally 40 mm in length, were all cored from the
1228 same set of blocks and in the same orientation. Samples were precision ground so that their end
1229 faces were flat and parallel. Prior to experimentation, samples were either: (1) held at ambient
1230 temperature (as-collected) or, (2) thermally stressed to pre-determined temperatures of 100, 200,
1231 300, 500, 750, or 1000 °C (note: NYT could not be tested after exposure to 1000 °C due to a
1232 severe volume reduction). Thermal stressing was achieved by heating the sample to the target
1233 temperature at a rate of 1 °C/min, holding the temperature constant for 60 minutes, and then
1234 cooling at the same rate. Once at room temperature, all samples were vacuum-saturated in

1235 distilled water prior to experimentation. The measured sample was then inserted into a nitrile
1236 rubber jacket and fixed between the two endcaps. The sample assembly was then lowered into
1237 the pressure vessel. Once inside the setup, the confining pressure (P_c) and the pore fluid
1238 (distilled water) **pressures (Pp)** in both the “upstream” (P_{up}) and “downstream” (P_{down}) pore
1239 volumometers were increased to 10 and 5 MPa, respectively. The confining and pore pressures
1240 were increased slowly to avoid damaging the sample, and care was taken to ensure the sample
1241 was not pressurised beyond the maximum effective pressure targeted for the experiments (5
1242 MPa). For the purpose of this study we apply the simple effective pressure law of $P_{eff} = P_c -$
1243 αP_p , assuming that poroelastic constant $\alpha = 1$ (Guéguen and Palciauskas, 1994). The sample was
1244 left for 30 minutes at an effective pressure of 5 MPa to ensure microstructural equilibration and
1245 complete saturation.

1246

1247 Once equilibration at $P_{eff} = 5$ MPa was complete, the first ultrasonic measurements were taken.
1248 Ultrasonic waves velocities were measured via PZT piezoelectric P- and S-wave transducer
1249 crystals housed in the sample endcaps (Figure 3) using an Agilent Technologies 1.5GHz
1250 “Infiniium” digital storage oscilloscope and a JSR DPR300 35MHz ultrasonic pulser/receiver.
1251 **All ultrasonic wave arrival times were individually picked as the first deviation from the baseline**
1252 **signal**. Dynamic elastic moduli were calculated from the resultant ultrasonic wave velocities
1253 using the following formulae (Guéguen and Palciauskas, 1994):

$$E_d = \rho \frac{V_s^2(3V_p^2 - 4V_s^2)}{V_p^2 - V_s^2} \quad (1)$$

1255

$$\nu_d = \frac{V_p^2 - 2V_s^2}{2(V_p^2 - V_s^2)} \quad (2)$$

1256

$$\mu_d = \frac{E_d}{2(1 + \nu_d)} \quad (3)$$

1257

1258 Where E_d is the Young's modulus, ν_d is the Poisson's ratio, μ_d is the shear modulus, ρ is the bulk
 1259 sample density and V_p and V_s are the P- and S-wave velocities, respectively.

1260

1261 Water permeability measurements were made by imposing a 1 MPa pressure difference across
 1262 the jacketed sample. To achieve this, P_{up} and P_{down} were set at 4.5 and 5.5 MPa, respectively. The
 1263 volumometers were then allowed to move full stroke (10 cm^3) and steady-state flow was only
 1264 assumed when the flow rate was constant over a protracted period. Water permeability (κ_{water})
 1265 was then calculated directly from Darcy's law:

1266

$$\frac{Q}{A} = \frac{\kappa_{water}}{\eta L} (P_{up} - P_{down}) \quad (4)$$

1267

1268 where Q is the fluid volume flux, A is the cross-sectional area of the sample, η is the viscosity of
 1269 the pore fluid (taken as $8.94 \times 10^{-4} \text{ Pa.s}$), L is the length of the sample, and P_{up} and P_{down} are the
 1270 pore pressures at the "upstream" and "downstream" ends of the sample, respectively.

1271

1272 Once the permeability measurement was complete, the "downstream" volumometer was isolated
 1273 and the "upstream" volumometer was set back at 5 MPa. The P_c was then slowly increased to 15
 1274 MPa. By monitoring the movement of the "upstream" volumometer the porosity change from

1275 Peff = 5 MPa to Peff = 10 MPa could be accurately calculated. The sample was then left for 30
1276 minutes at the new pressure to ensure microstructural equilibration. Once equilibration was
1277 complete, the ultrasonic measurements for Peff = 10 MPa were taken. This procedure was
1278 repeated for every 5 MPa Peff increment up to 50 MPa.

1279

1280 During our experiments, the length of the sample L and the cross-sectional area A will change
1281 due to the compaction of the sample at elevated pressure. We have corrected for this (in our
1282 calculations of permeability and ultrasonic wave velocities) using the volume reduction of our
1283 sample (as measured by the water expelled from the sample) at each pressure interval, assuming
1284 isotropic compaction. [Although one sample was used per thermal-stressing temperature, we](#)
1285 [reiterate that great care was taken during sample selection to exclude samples that contained](#)
1286 [large heterogeneities or anomalous connected porosities/P-wave velocities.](#)

1287

1288 3.2 Triaxial deformation experiments

1289

1290 Constant strain rate ($1.0 \times 10^{-5} \text{ s}^{-1}$) conventional (i.e., $\sigma_1 > \sigma_2 = \sigma_3$) triaxial experiments were
1291 performed on as-collected cylindrical samples of the two tuffs (20 mm in diameter and nominally
1292 40 mm in length). Samples were cored from the same blocks and in the same direction as for the
1293 [hydrostatic experiments described in the previous section](#). The samples were precision ground so
1294 that their end faces were flat and parallel. [Both](#) experiments were performed in the conventional
1295 triaxial deformation apparatus (Figure 4) at the Laboratoire de Déformation des Roches
1296 (Université de Strasbourg) at a Peff of 5 MPa (Pp of 5 MPa and a Pc of 10 MPa). Axial stress
1297 and strain were monitored continuously using a load cell and an LVDT displacement transducer,

1298 respectively. Pore volume change (used as a proxy for volumetric strain, ε_v) was monitored using
1299 a pore pressure intensifier, and the output of acoustic emissions (AEs) by a piezoelectric
1300 transducer crystal (located on the top of the piston) using a Physical Acoustics USB AE Node.
1301 AEs are high frequency elastic wave packets generated by the rapid release of strain energy such
1302 as during brittle microfracturing (see Lockner, 1993 for a review). During experimentation, an
1303 AE hit was recorded if a signal exceeded the set threshold of 40 dB. The AE “energy” (the area
1304 under the received AE waveform envelope) of each received AE signal was provided by the
1305 AEwin software. In this study we will adopt the convention that compressive stresses and
1306 compactive strains are positive.

1307
1308 Static Young’s moduli (E_s) and Poisson’s ratio (ν_s) were then calculated from the resultant
1309 stress-strain data, following the method of Heap and Faulkner (2008). We take both from the
1310 quasi-linear elastic regions of our tangent modulus curves (i.e., those regions where the moduli
1311 did not change). Static Poisson’s ratio is given by:

1312

$$\nu_s = - \frac{\varepsilon_r}{\varepsilon_a} \quad (5)$$

1313

1314 where

1315

$$\varepsilon_r = \frac{\varepsilon_v - \varepsilon_a}{2} \quad (6)$$

1316

1317 Where ε_r and ε_a are the radial and axial strain, respectively. Static shear modulus (μ_s) was then
1318 calculated using the following formula (Guéguen and Palciauskas, 1994):

1319

$$\mu_s = \frac{E_s}{2(1 + \nu_s)} \quad (7)$$

1320

1321 **3.3 Microstructural analyses**

1322

1323 Microstructural analyses were performed using (1) the Hitachi S-3600N Environmental Scanning
1324 Electron Microscope (E-SEM) at the University of Leicester using a working distance of 14.3
1325 mm and an accelerating voltage of 15 kV and, (2) a Leica DM2500 (equipped for both
1326 transmitted and reflected light) microscope with a mounted 5 megapixel Leica DFC425 digital
1327 camera (at the Laboratoire de Déformation des Roches, Université de Strasbourg). The E-SEM
1328 was used to look for evidence of pore collapse in samples of NYT taken beyond P^* . Optical
1329 microscopy was used to investigate the influence of high temperatures (1000 °C) on the
1330 microstructure of NYT and WGI.

1331

1332 **4. Results**

1333

1334 4.1 The evolution of porosity with increasing pressure and temperature

1335

1336 Plots of the evolution of porosity with increasing P_{eff} (commonly called “hydrostats”) for both
1337 NYT and WGI at each thermal stressing temperature are displayed in Figure 5. For porous rock,
1338 an increase in hydrostatic pressure results in a volume and porosity decrease. Initially, this
1339 compaction is elastic (i.e., recoverable) but, at some critical pressure (assuming the rock is
1340 porous enough), pore collapse and grain crushing (now non-recoverable damage) ensues and the

1341 rate of compaction accelerates. This critical pressure is denoted P^* (Wong and Baud, 2012). The
1342 P_{eff} required to reach P^* varies from rock to rock, but [depends largely](#) on the initial rock
1343 porosity and grain size (generally, the higher the porosity, the lower the P_{eff} for P^*). The stress
1344 at which P^* occurs can therefore provide important information on the physical and
1345 microstructural state of rock at depth. In our experiments, the position of P^* is about 10 MPa for
1346 NYT ([Figure 5A](#)) and about 10-15 MPa for WGI ([Figure 5B](#)). Prior to P^* , during elastic
1347 compaction, we note that the porosity change is linear (i.e., there is no concave portion that is
1348 usually attributed to the closure of microcracks; however this may be a result of the large steps in
1349 P_{eff} between measurements). [We note that](#) there is no microstructural evidence for microcracks
1350 in the as-collected materials (see Figure 2). Immediately following P^* , during inelastic
1351 compaction, there is a dramatic increase in the rate of porosity reduction, as inelastic compaction
1352 proceeds. However, the porosity reduction rate then gradually decreases (especially above about
1353 20 MPa). This represents the hardening of the rock due to compaction. Over the entire pressure
1354 range (up to 50 MPa) the porosity change for the as-collected sample is about the same for NYT
1355 and WGI (between 9 and 10 vol%). [Figure 5B](#) also shows that the porosity evolution for WGI
1356 with increasing P_{eff} is unaffected by thermal stressing. By contrast, in the case of NYT, the
1357 porosity change decreases significantly as thermal stressing temperature increases ([Figure 5A](#)). It
1358 can also be seen that, for both tuffs, thermal stressing does not appear to influence the position of
1359 P^* ([Figure 5](#)).

1360

1361 4.2 The evolution of permeability with increasing pressure and temperature

1362

1363 The evolution of permeability with increasing Peff for NYT and WGI at each thermal stressing
1364 temperature is displayed in Figure 6 (the values are reported in Tables 4 and 5). Firstly, we
1365 notice that the as-collected **permeabilities** of the two samples **are** very different. For instance, at a
1366 Peff of 5 MPa, the **permeabilities are** about 1.0×10^{-15} and 1.0×10^{-13} m² for NYT (Figure 6A)
1367 and WGI (Figure 6B), respectively.

1368

1369 For WGI, the permeability curves show little change between 5 and 15 MPa (Figure 6B).
1370 However, above 15 MPa, the permeability starts to decrease rapidly before reaching an apparent
1371 plateau above about 30 MPa. We note that this rapid decrease starts at the same pressure as the
1372 onset of inelastic compaction (P*). Overall, the permeability is reduced by about an order of
1373 magnitude from 1.0×10^{-13} m² at 5 MPa to 1.0×10^{-14} m² at 50 MPa. The permeability curves for
1374 WGI show no clear trend with increasing thermal stressing temperature (Figure 6B). The
1375 different values obtained for the different thermal stressing temperatures are within the expected
1376 range of natural variability between different samples cored from the same block.

1377

1378 However, there is a clear influence of the thermal stressing temperature on the permeability of
1379 NYT (Figure 6A). At a Peff of 5 MPa, the permeability increases from 1.0×10^{-15} m² for the as-
1380 collected sample to 1.1×10^{-14} m² for the sample thermally stressed to 750 °C, an increase of an
1381 order of magnitude. As for the WGI, the permeability curves show little change between 5 and
1382 10 MPa, after which permeability decreases more rapidly. We again note that this rapid decrease
1383 starts at the same pressure as the onset of inelastic compaction (P*). Over the entire pressure
1384 range, the permeability is reduced by about an order of magnitude for the as-collected sample
1385 and by about three orders of magnitude for the sample thermally stressed to 750 °C. Further, the

1386 total decrease in permeability increases with increasing thermal stressing temperature (Figure
1387 6A). The permeability curves all converge at about 40 MPa (at a permeability of about 4.0×10^{-17}
1388 m^2). Therefore, at Pe_{ff} s of 40 MPa and above, there is no longer any influence of thermal
1389 stressing on the permeability of NYT.

1390

1391 4.3 The evolution of ultrasonic velocities and dynamic elastic moduli with increasing pressure
1392 and temperature

1393

1394 The evolution of the tuff physical properties (ultrasonic wave velocities, dynamic elastic moduli,
1395 and Vp/Vs ratio) for NYT and WGI are shown in Figures 7 and 8, respectively. Firstly, it can be
1396 remarked that the as-collected physical properties of the two tuffs are similar (see also Table 1).

1397 For both tuffs, P- and S-wave velocity (Figures 7A, B and Figures 8A, B), dynamic Young's
1398 modulus (Figures 7C and 8C), dynamic Poisson's ratio (Figures 7D and 8D), dynamic shear
1399 modulus (Figures 7E and 8E) and Vp/Vs ratio (Figures 7F and 8F) all increase with increasing
1400 Pe_{ff} , and in a similar manner. For example, for the as-collected NYT sample, P-wave velocity
1401 increases by 40% (Figure 7A), S-wave velocity by 21% (Figure 7B), Young's modulus by 53%
1402 (Figure 7C), Poisson's ratio by 19% (Figure 7D), shear modulus by 47% (Figure 7E), and Vp/Vs
1403 ratio by 15% (Figure 7F) over the entire pressure range (5 to 50 MPa). The relative increases are
1404 similar for both tuffs. However, whereas the results for NYT (Figure 7) show a systematic
1405 decrease in all the physical properties with increasing thermal stressing temperature, no
1406 systematic pattern can be discerned in the WGI results (Figure 8). At a constant Pe_{ff} , thermal
1407 stressing decreases P- and S-wave velocity, dynamic Young's modulus, dynamic Poisson's ratio,
1408 and Vp/Vs ratio in NYT. For example, for NYT at a Pe_{ff} of 5 MPa, P-wave velocity decreases

1409 by 21% (Figure 7A), S-wave velocity by 4% (Figure 7B), Young's modulus by 18% (Figure 7C),
1410 Poisson's ratio by 56% (Figure 7D), shear modulus by 8% (Figure 7E), and Vp/Vs ratio by 17%
1411 (Figure 7F) over the entire temperature range (as-collected to 750 °C).

1412

1413 4.4 Static elastic moduli under triaxial conditions

1414

1415 The differential stress-axial strain curves and associated AE energy output curves for the triaxial
1416 experiments are shown in Figure 9, and the differential stress-porosity reduction curves are
1417 shown in Figure 10. Even at a P_{eff} as low as 5 MPa, the deformation behaviour of the two tuffs
1418 can be described as macroscopically ductile (i.e., their ability to resist load did not decrease, see
1419 Rutter, 1986). For both rocks, a critical pressure, termed C^* (Wong and Baud, 2012), is reached
1420 which marks the point where there is an acceleration in axial strain (Figure 9) and porosity
1421 reduction (or volumetric strain, Figure 10) for a given stress increment. This phenomenon is
1422 called "shear-enhanced compaction", and beyond C^* the rocks are deforming in the compactive,
1423 cataclastic flow regime which, in this case, is associated with strain hardening. In our
1424 experiments, C^* occurs at differential stresses of about 4.5 and 9 MPa for NYT (Figures 9A and
1425 10A) and WGI (Figures 9B and 10B), respectively. This contrasts with the values for P^* of 10
1426 and 15 MPa, respectively, and demonstrates how the application of shear stresses enhances
1427 compactive deformation. Although this mode of failure differs greatly from the brittle failure
1428 seen in the uniaxial experiments of Heap *et al.* (2012) on the same rocks, both deformation
1429 mechanisms involve the same micromechanical process: microcracking (as evidenced by the
1430 output of AE energy; a proxy for microcracking). However, whereas strain localisation is seen in
1431 the brittle field, cataclastic flow involves distributed microcracking (i.e., localisation does not

1432 occur). Indeed, we see no evidence for strain localisation in the post-experimental samples. The
1433 output of AE energy is seen to increase in a somewhat stepwise manner for both rocks (Figure
1434 9), reflecting bursts of microcracking events during deformation, we note that the average rate of
1435 AE energy output for WGI is some 20 times higher than for NYT. The difference in AE energy
1436 output during deformation is likely to be the result of the compositional differences between the
1437 two tuffs.

1438

1439 Values for the static Young's modulus, static Poisson's ratio, and static shear modulus were
1440 calculated from the elastic portions of the stress-strain curves and are given in Table 6, together
1441 with dynamic values determined at the same pressure ($P_{eff} = 5$ MPa) for comparison. We note
1442 that both the static Young's modulus and the static shear modulus are significantly lower than
1443 the corresponding dynamic values.

1444

1445 **5. Discussion**

1446

1447 5.1 Fluid flow and physical property evolution with depth

1448

1449 Our experimental data show that the water permeability of different as-collected tuff samples
1450 from Campi Flegrei can vary by multiple orders of magnitude (at a P_{eff} of 5 MPa, permeabilities
1451 are 1.0×10^{-15} and 1.0×10^{-13} m² for NYT and WGI, respectively). This difference in
1452 permeability could be considered surprising if one were to solely consider their connected
1453 porosities (44 and 49 vol% for NYT and WGI, respectively). The difference in permeability is
1454 likely due to differences in pore space connectivity, perhaps related to the extent of zeolitization

1455 and lithification. A similar conclusion was drawn by Vinciguerra *et al.* (2009). Vinciguerra *et al.*
1456 (2009) measured the permeability of two different tuffs from the Alban Hills (Italy) and found
1457 that, at a Peff of 5 MPa, the permeabilities of the two tuffs were significantly different. While the
1458 first (well-lithified, zeolitized facies with an average porosity of 14 vol.%) was found to have a
1459 permeability of about 10^{-18} m², which decreased by about an order of magnitude upon the
1460 application of a Peff of 70 MPa, the second (fine-grained, matrix-supported facies with frequent
1461 cm-sized accretionary lapilli and an average porosity of 18 vol.%) had a much higher
1462 permeability (about 10^{-15} m²) that decreased by about two orders of magnitude over the same
1463 pressure range. Further, considering the high porosities of NYT and WGI, their permeabilities
1464 are actually surprisingly low; considered to be a consequence of their complex pore structure. By
1465 contrast, Boise sandstone (porosity of 35 vol.%), a rock with a much simpler microstructure, has
1466 a permeability of 1.8×10^{-12} m² at a Peff of 5 MPa (Zhu and Wong, 1997).

1467
1468 Our experimental data also show that the permeability of the two tuffs is reduced by about an
1469 order of magnitude over the pressure range from 5 MPa to 50 MPa. In detail, the reduction in
1470 permeability with increasing Peff is modest up to a Peff of about 10-15 MPa, and accelerates at
1471 pressures above 10-15 MPa. This can be explained by the position of P* (Figure 5), the onset of
1472 inelastic pore collapse and grain crushing. As pores collapse and grains crushed, the pathways
1473 for fluid flow are obstructed. This inelastic compaction also has a significant influence on other
1474 physical properties of the tuffs (ultrasonic wave velocities, dynamic elastic moduli, and the
1475 Vp/Vs ratio all increase), in agreement with similar studies on NYT (Vanorio *et al.*, 2002;
1476 Vinciguerra *et al.*, 2006). Evidence of pore collapse is illustrated in the E-SEM image of a
1477 sample of NYT taken beyond P* provided as Figure 11. Pore collapse above P* has previously

1478 been observed in a tuff from the Alban Hills, Italy (Zhu *et al.*, 2011). A pressure of about 10-15
1479 MPa roughly equates to a depth of about 750 m. Geological cross sections of CF (e.g., Orsi *et al.*,
1480 1996) suggest therefore that a large volume of the NYT and WGI tuffs are located at depths
1481 where the pressure will be above P^* . This conjecture is confirmed by the reduced porosity of
1482 samples taken from borehole samples (see the report by Giberti *et al.*, 2006). Measurements on
1483 borehole samples from San Vito 1 (at the periphery of the inferred caldera) showed that the
1484 porosity decreases from 40.5 vol.% at the surface to 32.9, 21.9, 21.9, and 15.1 vol.% at depths of
1485 810, 1420, 2130, and 2860 m, respectively. Our data show that the porosity loss for NYT at 2860
1486 m will be about 9 vol.%. A starting porosity of 44 vol.% yields a porosity, purely due to
1487 mechanical compaction, of 35 vol.% at a depth of 2860 m. This would imply a porosity loss due
1488 to chemical alteration of about 20 vol.% and suggests that the impact of hot, circulating fluids
1489 plays the dominant role in the porosity loss of these pyroclastic deposits at depth. Indeed, the
1490 report by Giberti *et al.* (2006) suggests that it is the presence of clay minerals, rather than
1491 compaction, that is responsible for the major changes in porosity with depth.

1492
1493 We are certainly aware that our permeability data were collected on rocks from open quarries
1494 and, although their properties were measured at the relevant pressures (and under a range of
1495 thermal stressing temperatures), may not therefore accurately represent the material at depth
1496 (which have had time to compact, lithify, undergo chemical alteration; e.g., see de Gennaro *et*
1497 *al.*, 2000). However, the open access report of Giberti *et al.* (2006) offers some permeability data
1498 on borehole samples. Data from borehole samples taken from San Vito 1 (at the periphery of the
1499 inferred caldera) show that, as the porosity is reduced to 32.9, 21.9, 21.9, and 15.1 vol.% at
1500 depths of 810, 1420, 2130, and 2860 m, respectively, the permeability (Klinkenberg corrected

1501 gas permeabilities) of the samples are 1.1×10^{-13} , 2.5×10^{-16} , 7.9×10^{-16} , and $4.9 \times 10^{-16} \text{ m}^2$,
1502 respectively. The permeability of the quarry samples of this study are $8.0 \times 10^{-17} \text{ m}^2$ at a depth of
1503 about 2860 m. From these data it is clear that there is no simple relationship between the
1504 mechanical compaction and chemical alteration that afflicted the samples at depth (causing a
1505 substantial porosity loss) and their permeability.

1506

1507 5.2 The influence of temperature on fluid flow and physical properties

1508

1509 Our experimental data show that thermal stressing has a strong influence on the physical
1510 properties of NYT, whereas those for WGI are unaffected. The fluid flow properties of NYT are
1511 enhanced (especially at shallow depths) upon exposure to high temperatures, and the ultrasonic
1512 wave velocities, dynamic elastic moduli, and the V_p/V_s ratio decrease. Thermal stressing has
1513 previously shown to decrease ultrasonic wave velocities in a zeolitized tuff from CF
1514 (Vinciguerra *et al.*, 2006). The marked difference in the temperature-dependence of the physical
1515 properties between the two tuffs is likely due to the presence of significant quantities of
1516 thermally unstable zeolites in NYT, namely phillipsite and chabazite, which are not present in
1517 WGI (Heap *et al.*, 2012). Heap *et al.* (2012) showed, using a combination of thermo-gravimetric
1518 analysis, optical microscopy, and X-ray diffraction, that NYT lost 18% of its initial mass,
1519 contained large numbers of macrocracks, and no longer contained any zeolites after exposure to
1520 1000 °C. By contrast, no changes in mass, microstructure, or chemistry were seen in WGI heated
1521 to the same temperature (Heap *et al.*, 2012). Optical microscope photomicrographs of NYT and
1522 WGI thermally stressed to a temperature of 1000 °C are provided as Figures 12 and 13,
1523 respectively. Figure 12 shows that the microstructure of NYT is very different to that depicted in

1524 Figure 2B for the as-collected material. Many cracks are present (Figure 12A, B and C) and
1525 some areas contain 1 mm wide foamed glass (Figure 12A). By contrast, the microstructure of
1526 WGI, upon exposure to 1000 °C (Figure 13), is indistinguishable from the as-collected
1527 microstructure shown in Figure 2D. These observations have been previously reported in Heap *et*
1528 *al.* (2012). Since, phillipsite and chabazite represent the “cement” that promoted the lithification
1529 of the originally incoherent pozzolanic material constituting NYT (de Gennaro *et al.*, 2000), the
1530 structural integrity of NYT deteriorates significantly upon their loss (Heap *et al.*, 2012). Detailed
1531 studies (de Gennaro and Colella, 1989 and references therein) on the thermal decomposition of
1532 the zeolites in NYT have highlighted that analcime loses water irreversibly, and that chabazite
1533 and phillipsite undergo a partial reversible dehydration at 240 °C. Phillipsite breaks down during
1534 dehydration and chabazite undergoes reversible hydration at 350 °C, and, by 900 °C, the
1535 structure of the zeolites will be so damaged that no further water molecules can be stored (see de
1536 Gennaro and Colella, 1989 and references therein). Therefore, the reported changes in NYT
1537 physical properties are due to a combination of thermal cracking and the cracks formed as a
1538 result of the disintegration of the material through the loss of zeolites.

1539

1540 If we consider NYT at a depth of 1 km, the geothermal gradients provided by the AGIP (1987)
1541 exploration boreholes show that temperatures of 200-250 °C are not unreasonable (Wohletz *et*
1542 *al.*, 1999; de Lorenzo *et al.*, 2001). The data of this study reveal that the zeolitized NYT are
1543 prone to undesirable thermal alteration at these temperatures. At temperatures of 200-250 °C ,
1544 permeability increases by a factor of 2.5, ultrasonic wave velocities, dynamic elastic moduli, and
1545 Vp/Vs ratio decrease by roughly 10%; and uniaxial compressive strength and indirect tensile
1546 strength are reduced by more than a factor of 2 (Heap *et al.*, 2012). A reduction in tensile

1547 strength may further promote physical property changes by encouraging fluid pressure driven
1548 fracturing. An internal pore fluid pressure of 22-23 MPa (under a confining pressure of 6-7 MPa)
1549 was **sufficient** to fracture a sandstone of 13 vol.% porosity (Vinciguerra *et al.*, 2004). It is
1550 therefore likely that the estimated overpressures needed to explain the ground deformation at CF
1551 (e.g., 10 MPa, Gaeta *et al.*, 1998) are sufficient to fracture the tuffs and cause further changes in
1552 rock physical properties. **Although it has been shown that the porosity of borehole samples can**
1553 **be much less than those collected from the surface (see the report of Giberti *et al.*, 2006)** perhaps,
1554 **given their complex microstructure, it is unwise to assume that these rocks are stronger.** To
1555 **understand whether fluid driven fracturing is prevalent at CF, measurements of the tensile**
1556 **strength of samples taken from boreholes is required.**

1557

1558 5.3 Application of these data to ground deformation modelling at CF

1559

1560 **Our data highlight that the elastic moduli of two different tuffs from CF are significantly depth-**
1561 **dependent (Figures 7 and 8). The implication of these data is that the assumption of a**
1562 **homogenous half-space may be an oversimplification, and is exacerbated further when one**
1563 **considers the extent of the variability of the tuffs within the caldera (which are variably lithified,**
1564 **altered, and zeolitized, see the report of Giberti *et al.*, 2006).** These data highlight the need for
1565 **the development of more complex, multi-layer ground deformation models.** In order to assess the
1566 **extent of the variability in elastic moduli of the rocks within the caldera at CF, a systematic**
1567 **experimental approach involving borehole samples from different depths and locations within**
1568 **the caldera is now required** (discussed further at the end of the section).

1569

1570 We also find that static and dynamic moduli for the same tuff differ substantially. Although it is
1571 not uncommon for static and dynamic elastic moduli to be different, due to their frequency-
1572 dependence (Simmons and Brace, 1965; Cheng and Johnston, 1981; Eissa and Kazi, 1989;
1573 Ciccotti and Mulargia, 2004; Ciccotti *et al.*, 2004), it raises an important question regarding
1574 which values are more appropriate in modelling. Manconi *et al.* (2010) highlighted that, while
1575 dynamic elastic constants (those derived from seismic velocities) are representative for rock
1576 subject to a dynamic stress, perhaps static values are more appropriate in the analysis of
1577 deformation caused by volcanic sources. A similar conclusion was drawn by Heap *et al.* (2009).
1578 However, static elastic moduli for representative rocks at CF have not been available until now.
1579 Thus far, elastic moduli have been generally assumed, or extrapolated from seismic tomography
1580 studies (e.g., Chiarabba and Moretti, 2006). Typically, Poisson's ratio is taken as 0.3 and shear
1581 modulus as 5 GPa (e.g., De Natale *et al.*, 1991). However, while our data show that static and
1582 dynamic Poisson's ratio is similar for the measured tuffs (and equal to about 0.3; measurements
1583 on borehole samples are also consistently about 0.3, see the report by Giberti *et al.*, 2006), we
1584 also observe that the static shear modulus is about a factor of four lower than the dynamic value
1585 (Table 6). If one were to assume that our static values are representative, then a more suitable
1586 shear modulus would be 0.5 GPa, an order of magnitude lower than the values typically used in
1587 ground deformation modelling at CF. We note that, while values of the shear modulus of
1588 borehole samples provided in the report of Giberti *et al.* (2006) show that the dynamic shear
1589 modulus can reach values of 10.9 GPa at a depth of 2860 m, no complementary static values
1590 exist. Future research should focus on the determination of the static elastic moduli of borehole
1591 samples.

1592

1593 To date, the values of permeability used in the numerous thermodynamical and magmatic-
1594 hydrothermal models have spanned many orders of magnitude. For example, Gaeta *et al.* (1998)
1595 use a value of 10^{-11} m², inferred from the measurements of Ascolese *et al.* (1993a,b) and De
1596 Natale *et al.* (2001) use the same value, but inferred from the *in-situ* observations of Rosi and
1597 Sbrana (1987). By contrast, Gaeta *et al.* (2003) use a much lower value of 10^{-15} m², taken from
1598 the ambient pressure measurements of Peluso and Arienzzo (2007). The experimental data of this
1599 study has shown that (1) the permeability of tuffs at CF can differ by about 1.5 orders of
1600 magnitude (from 2.0×10^{-15} to 6.3×10^{-17} m², due to the extent of zeolitization and lithification,
1601 see Tables 4 and 5), (2) effective pressure (depth) can significantly alter the permeability of tuff
1602 (by up to two orders of magnitude, see Figure 6) and, (3) if the tuff is zeolitized, permeability
1603 can be increased by thermal stressing episodes (Figure 6A). While we note that the permeability
1604 of different tuffs at CF can differ greatly (we expect the extent of the variation to greatly exceed
1605 the 1.5 orders of magnitude quoted here), the same will also be true for tuff from the same
1606 eruptive episode. The NYT and the Campanian Ignimbrite – both thick and widespread
1607 pyroclastic deposits – are well-known to be variably lithified and zeolitized (de Gennaro *et al.*,
1608 2000; Langella *et al.*, 2013). The highly variable nature of tuffs at CF (both laterally and
1609 vertically, see the report by Giberti *et al.*, 2006), coupled with the depth-dependence of
1610 permeability, is likely to produce highly variable permeabilities within the caldera.
1611 Unfortunately, the implication of this conclusion is that, to accurately model ground deformation
1612 using a model that requires an estimation of the permeability of the materials within the caldera,
1613 we now require (1) permeability measurements on borehole samples (from different depths and
1614 different locations within the caldera) to assess the extent of the variability in permeability within

1615 the caldera and, (2) the development of more complex models that can account for such
1616 variations in permeability.

1617

1618 To conclude, while we advise that our laboratory-derived values should be considered for routine
1619 ground deformation modelling at CF, we also urge caution. Firstly, our measurements on
1620 laboratory-sized samples do not account for large faults or fractures, which, for example, would
1621 serve to lower the Young's modulus. Secondly, an important question arises: what constitutes
1622 "representative" materials for the caldera at CF? Although our experiments were conducted (1)
1623 on samples from the two most widespread tuff lithologies that comprise CF, (2) under the
1624 relevant pressures or depths, (3) on water-saturated samples and, (4) over a range of thermal
1625 stressing temperatures, our samples were collected from an open quarry and may therefore not
1626 represent the material at depth (which have had time to compact, lithify, undergo chemical
1627 alteration; e.g., see de Gennaro *et al.*, 2000; see also the report by Giberti *et al.*, 2006). However,
1628 we highlight that the permeability measurements on borehole samples presented in the report of
1629 Giberti *et al.* (2006) suggest that (1) the permeability measurements of this study are not
1630 dissimilar to those measured on borehole samples and, (2) there is clearly no simple relationship
1631 between porosity and permeability. Further, the tuffs of CF are likely to be extremely variable
1632 (due to variable lithification, zeolitization, interaction with fluids and temperatures) laterally (i.e.,
1633 within the same lithological unit) and therefore their physical properties at a constant depth are
1634 also likely to span a wide range. It is clear that systematic measurements on deep scientific
1635 borehole samples are now needed from multiple locations and depths within the caldera to assess
1636 the extent of the variability in static elastic moduli and permeability of the rocks that form the
1637 caldera. To conclude, we anticipate that no unique values of permeability or elastic moduli exist

1638 for the materials within CF, highlighting the need for the development of more complex ground
1639 deformation models.

1640

1641 **6. Conclusions**

1642

1643 1. Our experimental data show that the permeabilities of tuffs from Campi Flegrei (the
1644 Neapolitan Yellow Tuff and a tuff from the Campanian Ignimbrite) can vary by multiple
1645 orders of magnitude. Despite this, our data also show that their elastic moduli are similar;
1646 however, we note that dynamic and static moduli differ greatly. These data emphasize the
1647 heterogeneous nature of the tuffs that comprise the caldera at Campi Flegrei.

1648 2. Increasing the effective pressure from 5 MPa to 50 MPa results in a permeability
1649 reduction of about an order of magnitude and a porosity reduction between 5 and 10
1650 vol.% for both tuffs. As effective pressure increases we also observe an increase in
1651 ultrasonic wave velocities, dynamic elastic moduli, and Vp/Vs ratio. These changes all
1652 accelerate after the onset inelastic pore collapse (P^*), which exists between effective
1653 pressures of 10-15 MPa.

1654 3. Thermal stressing increases the permeability and decreases the ultrasonic wave velocities,
1655 dynamic elastic moduli, and Vp/Vs ratio of the Neapolitan Yellow Tuff. However, the
1656 tuff from the Campanian Ignimbrite is unaffected by thermal stressing. This is the result
1657 of the loss of thermally unstable zeolites, namely phillipsite and chabazite, in Neapolitan
1658 Yellow Tuff. For example, for the sample thermally stressed to 750 °C, the permeability
1659 at an effective pressure of 5 MPa increases by an order of magnitude relative to the as-
1660 collected material.

1661 4. While we urge that these new laboratory data should be considered in routine ground
1662 deformation modelling, our study highlights that the physical properties of just two rocks
1663 that comprise the caldera at Campi Flegrei can be extremely heterogeneous (we also
1664 anticipate that future measurements will further expand our knowledge of such
1665 heterogeneity). These data underline the challenges for accurate ground deformation
1666 modelling at Campi Flegrei. We anticipate that no unique values of permeability or
1667 elastic moduli exist for the materials within Campi Flegrei, highlighting the need for the
1668 development of more complex ground deformation models.

1669

1670 **Acknowledgements**

1671

1672 We gratefully acknowledge John Bowles, Steve Boon and Neil Hughes (all UCL) for help and
1673 support during experimentation. We thank G. Orsi for the provision of the experimental
1674 materials, and Y. Lavallée for discussions. M. J. Heap acknowledges CNRS INSU grant “*Étude*
1675 *de la stabilité des édifices volcaniques*”. P. Baud and P. G. Meredith acknowledge the support of
1676 a CNRS PICS grant. The reviews of Andrea Manconi, Claudia Cannatelli, Maurizio de Gennaro,
1677 one anonymous reviewer, and comments by the editor (Antonella Longo), greatly improved this
1678 manuscript.

1679

1680 **Table 1.** Summary of the ambient pressure, as-collected physical properties of Neapolitan
 1681 Yellow Tuff (NYT) and Grey Campanian Ignimbrite (WGI). “Dry” indicates measurements on
 1682 samples that were dried in a vacuum oven for at least 24 hours; the measurements were then
 1683 performed under ambient laboratory humidity. “Wet” indicates measurements on samples that
 1684 were vacuum-saturated with distilled water.

	Neapolitan Yellow Tuff (NYT)	Grey Campanian Ignimbrite (WGI)
connected porosity [vol.%]	43.8	48.5
dry bulk sample density [kg/m³]	1270	1330
dry P-wave velocity [kms⁻¹]	2.29	2.31
wet P-wave velocity [kms⁻¹]	2.60	2.56
dry S-wave velocity [kms⁻¹]	1.25	1.28
wet S-wave velocity [kms⁻¹]	1.30	1.33
dry Vp/Vs	1.84	1.80
wet Vp/Vs	2.00	1.93
dry dynamic Young’s modulus [GPa]	5.07	5.58
wet dynamic Young’s modulus [GPa]	7.68	8.42
dry dynamic Poisson’s ratio	0.28	0.28
wet dynamic Poisson’s ratio	0.33	0.31
dry dynamic shear modulus [GPa]	1.97	2.19
wet dynamic shear modulus [GPa]	2.88	3.20
dry unconfined compressive strength [MPa] (from Heap et al., 2012)	3.47	9.23

1685

1686

1687

Table 2. Summary of the estimated measurement accuracy.

measurement	accuracy
confining pressure [Pa]	$\pm 100\,000$ (UCL) $\pm 10\,000$ (Strasbourg)
pore fluid pressure [Pa]	$\pm 10\,000$
pore fluid volume [m³]	$\pm 1.0 \times 10^{-12}$
LVDT displacement [m]	± 0.000001
axial stress [Pa]	$\pm 10\,000$
original sample dimensions [m]	± 0.00001

1688

1689

1690 **Table 3.** Expected natural variability between tuff samples cored from the same block. Note that
 1691 these are not “errors” in the measurements. Measurement accuracies (Table 2) are insignificant
 1692 compared to the natural sample variability, despite efforts to reduce the variability between
 1693 samples cored from the same block of material (see text for details).

	expected natural variability
Young’s modulus [GPa]	± 0.5
Poisson’s ratio	± 0.05
shear modulus [GPa]	± 0.5
water permeability [m²]	$\pm 1.0 \times 10^{-14}$
P-wave velocity [kms⁻¹]	± 0.1
S-wave velocity [kms⁻¹]	± 0.1

1694

1695 **Table 4.** Water permeability of Neapolitan Yellow Tuff (NYT) as a function of effective
 1696 pressure and thermal stressing temperature.

Neapolitan Yellow Tuff (NYT)						
effective pressure [MPa]	“as-collected” permeability [m ²]	100 °C permeability [m ²]	200 °C permeability [m ²]	300 °C permeability [m ²]	500 °C permeability [m ²]	750 °C permeability [m ²]
5	1.2×10^{-15}	1.7×10^{-15}	1.9×10^{-15}	2.7×10^{-15}	4.1×10^{-15}	1.1×10^{-14}
10	8.5×10^{-16}	1.7×10^{-15}	2.0×10^{-15}	2.7×10^{-15}	3.6×10^{-15}	1.1×10^{-14}
15	6.3×10^{-16}	1.6×10^{-15}	1.6×10^{-15}	2.4×10^{-15}	2.5×10^{-15}	8.5×10^{-15}
20	4.9×10^{-16}	1.1×10^{-15}	8.2×10^{-16}	1.6×10^{-15}	1.5×10^{-15}	6.1×10^{-15}
25	2.5×10^{-16}	7.6×10^{-16}	4.5×10^{-16}	1.2×10^{-15}	8.0×10^{-16}	4.4×10^{-15}
30	1.7×10^{-16}	5.3×10^{-16}	2.5×10^{-16}	8.6×10^{-16}	4.8×10^{-16}	3.2×10^{-15}
35	8.0×10^{-17}	5.3×10^{-16}	1.4×10^{-16}	6.4×10^{-16}	3.0×10^{-16}	1.8×10^{-15}
40	4.7×10^{-17}	3.1×10^{-16}	9.6×10^{-17}	5.3×10^{-16}	2.7×10^{-16}	3.1×10^{-16}
45	3.5×10^{-17}	2.3×10^{-16}	6.0×10^{-17}	4.1×10^{-16}	1.5×10^{-16}	5.4×10^{-17}
50	2.4×10^{-17}	1.7×10^{-16}	4.0×10^{-17}	3.2×10^{-16}	1.0×10^{-16}	3.3×10^{-17}

1697

1698

1699 **Table 5.** Water permeability of grey Campanian Ignimbrite (WGI) as a function of effective
 1700 pressure and thermal stressing temperature.

Grey Campanian Ignimbrite (WGI)							
effective pressure [MPa]	“as-collected” permeability [m ²]	100 °C permeability [m ²]	200 °C permeability [m ²]	300 °C permeability [m ²]	500 °C permeability [m ²]	750 °C permeability [m ²]	1000 °C permeability [m ²]
5	1.0 x 10 ⁻¹³	7.8 x 10 ⁻¹⁴	1.1 x 10 ⁻¹³	1.0 x 10 ⁻¹³	1.0 x 10 ⁻¹³	1.0 x 10 ⁻¹³	9.9 x 10 ⁻¹⁴
10	9.7 x 10 ⁻¹⁴	7.8 x 10 ⁻¹⁴	1.1 x 10 ⁻¹³	1.0 x 10 ⁻¹³	9.7 x 10 ⁻¹⁴	1.0 x 10 ⁻¹³	9.4 x 10 ⁻¹⁴
15	8.9 x 10 ⁻¹⁴	6.8 x 10 ⁻¹⁴	9.2 x 10 ⁻¹⁴	9.5 x 10 ⁻¹⁴	7.8 x 10 ⁻¹⁴	9.8 x 10 ⁻¹⁴	8.2 x 10 ⁻¹⁴
20	7.4 x 10 ⁻¹⁴	3.8 x 10 ⁻¹⁴	6.7 x 10 ⁻¹⁴	8.4 x 10 ⁻¹⁴	4.9 x 10 ⁻¹⁴	8.4 x 10 ⁻¹⁴	6.2 x 10 ⁻¹⁴
25	5.3 x 10 ⁻¹⁴	2.4 x 10 ⁻¹⁴	2.4 x 10 ⁻¹⁴	6.3 x 10 ⁻¹⁴	2.7 x 10 ⁻¹⁴	4.0 x 10 ⁻¹⁴	4.4 x 10 ⁻¹⁴
30	2.5 x 10 ⁻¹⁴	1.5 x 10 ⁻¹⁴	8.6 x 10 ⁻¹⁵	4.8 x 10 ⁻¹⁴	1.4 x 10 ⁻¹⁴	2.0 x 10 ⁻¹⁴	3.2 x 10 ⁻¹⁴
35	1.3 x 10 ⁻¹⁴	1.2 x 10 ⁻¹⁴	5.7 x 10 ⁻¹⁵	3.7 x 10 ⁻¹⁴	8.0 x 10 ⁻¹⁵	1.2 x 10 ⁻¹⁴	2.4 x 10 ⁻¹⁴
40	7.9 x 10 ⁻¹⁵	8.6 x 10 ⁻¹⁵	4.6 x 10 ⁻¹⁵	2.4 x 10 ⁻¹⁴	5.5 x 10 ⁻¹⁵	8.7 x 10 ⁻¹⁵	1.9 x 10 ⁻¹⁴
45	4.5 x 10 ⁻¹⁵	6.0 x 10 ⁻¹⁵	4.0 x 10 ⁻¹⁵	1.9 x 10 ⁻¹⁴	4.0 x 10 ⁻¹⁵	6.6 x 10 ⁻¹⁵	1.4 x 10 ⁻¹⁴
50	2.2 x 10 ⁻¹⁵	4.2 x 10 ⁻¹⁵	3.5 x 10 ⁻¹⁵	1.3 x 10 ⁻¹⁴	3.0 x 10 ⁻¹⁵	5.5 x 10 ⁻¹⁵	1.1 x 10 ⁻¹⁴

1701

1702 **Table 6.** The static and dynamic elastic moduli of Neapolitan Yellow Tuff (NYT) and Grey
1703 Campanian Ignimbrite (WGI) measured under an effective pressure of 5 MPa.

	Neapolitan Yellow Tuff (NYT)		Grey Campanian Ignimbrite (WGI)	
	static	dynamic	static	dynamic
Young's modulus [GPa]	2.1	6.0	1.7	4.9
Poisson's ratio	0.30	0.31	0.29	0.24
shear modulus [GPa]	0.81	3.1	0.66	2.7

1704

1705

1706 **Figure captions**

1707

1708 **Figure 1.** Map showing the location of the inferred Campi Flegrei caldera and the proximity of
1709 Naples to both the Campi Flegrei caldera and Mt. Vesuvius. The Neapolitan Yellow Tuff used in
1710 this study was sourced from an open quarry within the inferred CF caldera at Monte San
1711 Severino (i.e., within the red circle in Figure 1), while the Grey Campanian Ignimbrite was
1712 sourced from an open quarry to the north-west of the town of Caserta (the blocks used in this
1713 study are the same as those used in Heap *et al.*, 2012).

1714

1715 **Figure 2.** Photographs and optical microscopy images of the as-collected Neapolitan Yellow
1716 Tuff (A and B) and Grey Campanian Ignimbrite (C and D). The photomicrographs are taken
1717 from Heap *et al.* (2012).

1718

1719 **Figure 3.** Schematic diagram of the permeameter at the Rock & Ice Physics Laboratory (RIPL),
1720 University College London. Schematic is not to scale.

1721

1722 **Figure 4.** Schematic diagram of the triaxial deformation apparatus at the Laboratoire de
1723 Déformation des Roches, Université de Strasbourg. Schematic is not to scale.

1724

1725 **Figure 5.** The evolution of porosity change with increasing effective pressure for Neapolitan
1726 Yellow Tuff (A) and Grey Campanian Ignimbrite (B). The temperatures in the legend refer to the
1727 thermal stressing temperature (see text for details).

1728

1729 **Figure 6.** The evolution of water permeability with increasing effective pressure for Neapolitan
1730 Yellow Tuff (A) and Grey Campanian Ignimbrite (B). The temperatures in the legend refer to the
1731 thermal stressing temperature (see text for details).

1732

1733 **Figure 7.** The evolution of P-wave velocity (A), S-wave velocity (B), dynamic Young's modulus
1734 (C), dynamic Poisson's ratio (D), dynamic shear modulus (E), and Vp/Vs ratio (F) with
1735 increasing effective pressure for Neapolitan Yellow Tuff. The temperatures in the legend refer to
1736 the thermal stressing temperature (see text for details).

1737

1738 **Figure 8.** The evolution of P-wave velocity (A), S-wave velocity (B), dynamic Young's modulus
1739 (C), dynamic Poisson's ratio (D), dynamic shear modulus (E), and Vp/Vs ratio (F) with
1740 increasing effective pressure for Grey Campanian Ignimbrite. The temperatures in the legend
1741 refer to the thermal stressing temperature (see text for details).

1742

1743 **Figure 9.** Constant strain rate stress-strain curves, together with the cumulative output of
1744 acoustic emission (AE) "energy" (the area under the received AE waveform envelope) for as-
1745 collected Neapolitan Yellow Tuff (A) and Grey Campanian Ignimbrite (B). The experimental
1746 conditions are provided on each panel and the positions of C* are indicated by the arrows. The
1747 steps in the data are due to the stepwise nature of the pumps.

1748

1749 **Figure 10.** Constant strain rate stress-porosity reduction curves for as-collected Neapolitan
1750 Yellow Tuff (A) and Grey Campanian Ignimbrite (B). The experiments shown here are the same

1751 as those in Figure 9. The experimental conditions are provided on each panel and the positions of
1752 C^* are indicated by the arrows. The steps in the data are due to the stepwise nature of the pumps.

1753

1754 **Figure 11.** Scanning electron microscope images of an as-collected sample of Neapolitan
1755 Yellow Tuff taken beyond P^* . **Panel A** shows an overview of the post- P^* microstructure at a low
1756 **magnification**. Panels B and C show **detailed** evidence of pore collapse (**indicated by the white**
1757 **arrows**). Panel C is a zoom of the white box shown in panel B.

1758

1759 **Figure 12.** Optical microscope images of Neapolitan Yellow Tuff thermally stressed to a
1760 temperature of 1000 °C showing macrocracks. The photomicrograph in panel A, showing
1761 foaming, is taken from Heap *et al.* (2012).

1762

1763 **Figure 13.** Optical microscope images of grey Campanian Ignimbrite thermally stressed to a
1764 temperature of 1000 °C. Both photographs are taken from Heap *et al.* (2012).

1765

1766 **References**

1767
1768 AGIP, Geologia e Geofisica Del Sistema Geotermico Dei Campi Flegrei, Servizi Centrali per l'Esplorazione,
1769 SERG-MMESG, San Donato, 1987.

1770
1771 Ascolese, E., Aurisicchio, A., Briggs-Smith, M., Mita, D. G., Perna, G., Rossi, S. and Gaeta, F. S., 1993.
1772 Thermodynamics of water-permeated unwelded pyroclasts, 1: equilibrium properties, *Journal of*
1773 *Volcanology and Geothermal Research*, **57**, 219-233.

1774
1775 Ascolese, E., Aurisicchio, A., Briggs-Smith, M., Mita, D. G., Perna, G., Rossi, S. and Gaeta, F. S., 1993.
1776 Thermodynamics of water-permeated unwelded pyroclasts, 2: non-equilibrium properties, *Journal of*
1777 *Volcanology and Geothermal Research*, **59**, 235-251.

1778
1779 Barberi, E., Cassano, E., La Torre, P. and Sbrana, A., 1991. Structural evolution of Campi Flegrei caldera in
1780 light of volcanological and geophysical data, *Journal of Volcanology and Geothermal Research*, **48**, 33-49.

1781
1782 Battaglia, M., Troise, C., Obrizzo, F., Pingue, F. and De Natale, G., 2006. Evidence for fluid migration as
1783 the source of deformation at Campi Flegrei caldera (Italy), *Geophysical Research Letters*, **33**, L01307,
1784 doi:10.1029/2005GL024904.

1785
1786 Beauducel, F., De Natale, G., Obrizzo, F. and Pingue, F., 2004. 3-D Modelling of Campi Flegrei Ground
1787 Deformations: Role of Caldera Boundary Discontinuities, *Pure and Applied Geophysics*, **161**, 1329-1344.

1788
1789 Berrino, G., Corrado, G., Luongo, G. and Toro, B., 1984. Ground deformation and gravity changes
1790 accompanying the 1982 Pozzuoli uplift, *Bulletin of Volcanology*, **47**, 187-200.

1791
1792 Bianchi, R., Coradini, A., Federico, C., Giberti, G., Lanciano, P., Pozzi, J. P., Sartoris, G. and Scandone, R.,
1793 1987. Modeling of Surface Deformation in Volcanic Areas: The 1970–1972 and 1982–1984 Crises of
1794 Campi Flegrei, Italy, *Journal of Geophysical Research*, **92**, 14139-14150.

1795
1796 Bianco, F., Del Pezzo, E., Saccorotti, G. and Ventura, G., 2004. The role of hydrothermal fluids in
1797 triggering the July–August 2000 seismic swarm at Campi Flegrei, Italy: evidence from seismological and
1798 mesostructural data, *Journal of Volcanology and Geothermal Research*, **133**, 229-246.

1799
1800 Bodnar, R. J., Cannatelli, C., De Vivo, B., Lima, A., Belkin, H. E. and Milia, A., 2007. Quantitative model for
1801 magma degassing and ground deformation (bradyseism) at Campi Flegrei, Italy: Implications for future
1802 eruptions, *Geology*, **35**, 791-794.

1803
1804 Bonafede, M., 1991. Hot fluid migration: an efficient source of ground deformation: application to the
1805 1982–1985 crisis at Campi Flegrei-Italy, *Journal of Volcanology and Geothermal Research*, **48**, 187-198.

1806
1807 Bonafede, M., Dragoni, M. and Quarenii, F., 1986. Displacement and stress fields produced by a centre of
1808 dilation and by a pressure source in a viscoelastic half space: application to the study of ground
1809 deformation and seismic activity at Campi Flegrei, Italy, *Geophysical Journal International*, **87**, 455-485.

1810
1811 Bonafede, M. and Mazzanti, M., 1998. Modelling gravity variations consistent with ground deformation
1812 in the Campi Flegrei caldera (Italy), *Journal of Volcanology and Geothermal Research*, **81**, 137-157.

1813
1814 Cappelletti, P., Cerri, G., Collettini, C., de Gennaro, M., Langella, A., Perrotta, A. and Scarpati, C., 2003.
1815 Post-eruptive processes in the Campanian Ignimbrite, *Mineralogy and Petrology*, **79**, 79-97.
1816
1817 Cheng, C. H. and Johnston, D. H., 1981. Dynamic and static moduli, *Geophysical Research Letters*, **8**, 39-
1818 42.
1819
1820 Chiarabba, C. and Moretti, M., 2006. An insight into the unrest phenomena at the Campi Flegrei caldera
1821 from Vp and Vp/Vs tomography, *Terra Nova*, **18**, 373-379, doi: 10.1111/j.1365-3121.2006.00701.x.
1822
1823 Chiodini, G., Caliro, S., De Martino, P., Avino, R. and Gherardi, F., 2012. Early signals of new volcanic
1824 unrest at Campi Flegrei caldera? Insights from geochemical data and physical simulations, *Geology*, **40**,
1825 943-946.
1826
1827 Chiodini, G., Todesco, M., Caliro, S., Del Gaudio, C., Macedonio, G. and Russo, M., 2003. Magma
1828 degassing as a trigger of bradyseismic events: The case of Phleorean Fields (Italy), *Geophysical Research
1829 Letters*, **30**, No. 8, 1434, doi: 10.1029/2002GL016790.
1830
1831 Chiodini, G., Vilardo, G., Augusti, V., Granieri, D., Caliro, S., Minopoli, C. and Terranova, C., 2007. Thermal
1832 monitoring of hydrothermal activity by permanent infrared automatic stations: Results obtained at
1833 Solfatara di Pozzuoli, Campi Flegrei (Italy), *Journal of Geophysical Research*, **112**, B12206,
1834 doi:10.1029/2007JB005140.
1835
1836 Ciccotti, M., Almagro, R. and Mularia, F., 2004. Static and dynamic moduli of the seismogenic layer in
1837 Italy, *Rock Mechanics and Rock Engineering*, **37**(3), 229-238.
1838
1839 Ciccotti, M. and Mularia, F., 2004. Differences between static and dynamic elastic moduli of a typical
1840 seismogenic rock, *Geophysical Journal International*, **157**, 474-477.
1841
1842 D'Auria, L., Giudicepietro, F., Aquino, I., Borriello, G., Del Gaudio, C., Lo Bascio, D., Martini, M., Ricciardi,
1843 G. P., Ricciolino, P. and Ricco, C., 2011. Repeated fluid-transfer episodes as a mechanism for the recent
1844 dynamics of Campi Flegrei caldera (1989–2010), *Journal of Geophysical Research*, **116**, DOI:
1845 10.1029/2010JB007837.
1846
1847 David, C., Menéndez, B. and Darot, M., 1999. Infuence of stress-induced and thermal cracking on
1848 physical properties and microstructure of La Peyratte granite, *International Journal of Rock Mechanics
1849 and Mining Sciences*, **36**, 433-448.
1850
1851 de Gennaro, M., Cappelletti, P., Langella, A., Perrotta, A. and Scarpati, C., 2000. Genesis of zeolites in the
1852 Neapolitan Yellow Tuff: geological, volcanological and mineralogical evidences., *Contributions to
1853 Mineralogy and Petrology*, **139**, 17-35.
1854
1855 de Gennaro, M. and Colella, C., 1989. Use of thermal analysis for the evaluation of zeolite content in
1856 mixtures of hydrated phases, *Thermochimica Acta*, **154**, 345-353.
1857
1858 de Gennaro, M., Petrosino, S., Conte, M. T., Munno, R. and Colella, A., 1990. Zeolite chemistry and
1859 distribution in a Neapolitan Yellow Tuff deposit, *Eur. J. Mineral.*, **2**, 779-786.
1860

1861 de Lorenzo, S., Gasparini, P., Mongelli, F. and Zollo, A., 2001. Thermal state of the Campi Flegrei caldera
1862 inferred from seismic attenuation tomography, *Journal of Geodynamics*, **32**, 467-486.

1863

1864 De Natale, G. and Pingue, F., 1993. Ground deformations in collapsed caldera structures, *Journal of*
1865 *Volcanology and Geothermal Research*, **57**, 19-38.

1866

1867 De Natale, G., Troise, C. and Pingue, F., 2001. A mechanical fluid-dynamical model for ground
1868 movements at Campi Flegrei caldera, *Journal of Geodynamics*, **32**, 487-517.

1869

1870 De Natale, G., Troise, C., Pingue, F., Mastrolorenzo, G., Pappalardo, L., Battaglia, M. and Boschi, E., 2006.
1871 The Campi Flegrei caldera: Unrest mechanisms and hazards, *Geol. Soc. London, Special Publications*, **269**,
1872 25-45.

1873

1874 De Vivo, B., Rolandi, G., Gans, P. B., Calvert, A., Bohrson, W. A., Spera, F. J. and Belkin, H. E., 2001. New
1875 constraints on the pyroclastic eruptive history of the Campanian volcanic Plain (Italy), *Mineralogy and*
1876 *Petrology*, **73**, 47-65.

1877

1878 Deino, A. L., Orsi, G., De Vita, S. and Piochi, M., 2004. The age of the Neapolitan Yellow Tuff caldera-
1879 forming eruption (Campi Flegrei caldera - Italy) assessed by
1880 40Ar/39Ar dating method, *Journal of Volcanology and Geothermal Research*, **133**, 157-170.

1881

1882 Dzurisin, D., 2006. Volcano Deformation, Chichester, U.K., Springer. ISBN: 978-3540426424.

1883

1884 Eissa, E. A. and Kazi, A., 1989. Relation between static and dynamic Young's moduli of rocks,
1885 *International Journal of Rock Mechanics and Mining Sciences and Geomechanics Abstracts*, **25**, 479-482.

1886

1887 Gaeta, F. S., De Natale, G., Peluso, F., Mastrolorenzo, G., Castagnolo, D., Troise, C., Pingue, F., Mita, D. G.
1888 and Rossano, S., 1998. Genesis and evolution of unrest episodes at Campi Flegrei caldera: The role of
1889 thermal fluid-dynamical processes in the geothermal system, *Journal of Geophysical Research*, **103**,
1890 20921-20933.

1891

1892 Gaeta, F. S., Peluso, F., Arienzo, I., Castagnolo, D., De Natale, G., Milano, G., Albanese, C. and Mita, D. G.,
1893 2003. A physical appraisal of a new aspect of bradyseism: The miniuplifts, *Journal of Geophysical*
1894 *Research*, **108**, No. B8, 2363, doi:10.1029/2002JB001913.

1895

1896 Giberti, G., Yven, B., Zamora, M. and Vanorio, T., 2006. Database on laboratory measured data on
1897 physical properties of rocks of Campi Flegrei volcanic area (Italy). In: *Geophysical Exploration of the*
1898 *Campi Flegrei (Southern Italy) Caldera' Interiors: Data, Methods and Results*, edited by A. Zollo, P.
1899 Capuano and M. Corciulo, Doppiaovoce, Naples. ISBN-10: 88-89972-04-1, ISBN-13: 978-88-89972-04-5.

1900

1901 Gottsmann, J., Camacho, A. G., Tiampo, K. F. and Fernandez, J., 2006. Spatiotemporal variations in
1902 vertical gravity gradients at the Campi Flegrei caldera (Italy): A case for source multiplicity during
1903 unrest?, *Geophysical Journal International*, **167**, 1089-1096.

1904

1905 Guéguen, Y. and Palciauskas, V., 1994. Introduction to the Physics of Rocks, Princeton University Press,
1906 Princeton, New Jersey, ISBN: 9780691034522.

1907

1908 Heap, M. J., Lavallée, Y., Laumann, A., Hess, K.-U., Meredith, P. G. and Dingwell, D. B., 2012. How tough
1909 is tuff in the event of fire?, *Geology*, **40**, 311-314.

1910

1911 Homand-Etienne, F. and Troalen, J.-P., 1984. Behaviour of granites and limestones subjected to slow and
1912 homogenous temperature changes, *Engineering Geology*, **20**, 219-233.

1913

1914 Hurwitz, S., Christiansen, L. B. and Hsieh, P. A., 2007. Hydrothermal fluid flow and deformation in large
1915 calderas: Inferences from numerical simulations, *Journal of Geophysical Research*, **112**, B02206,
1916 doi:10.1029/2006JB004689.

1917

1918 Jones, C., Keaney, G., Meredith, P. G. and Murrell, S. A. F., 1997. Acoustic Emission and Fluid
1919 Permeability Measurements on Thermally Cracked Rocks, *Phys. Chem. Earth*, **22**, No. 1-2, 13-17.

1920

1921 Keshavarz, M., Pellet, F. L. and Loret, B., 2010. Damage and Changes in Mechanical Properties of a
1922 Gabbro Thermally Loaded up to 1,000°C, *Pure and Applied Geophysics*, **167**, 1511-1523.

1923

1924 Kolzenburg, S., Heap, M. J., Lavallée, Y., Russell, J. K. R., Meredith, P. G. and Dingwell, D. B., 2012.
1925 Strength and permeability recovery of tuffisite-bearing andesite, *Solid Earth*, **3**, 191-198.

1926

1927 Lanari, R., Berardino, P., Borgstrom, S., Del Gaudio, C., De Martino, P., Fornaro, G., Guarino, S., Ricciardi,
1928 G. P., Sansosti, E. and Lundgren, P., 2004. The use of IFSAR and classical geodetic techniques for caldera
1929 unrest episodes: application to the Campi Flegrei uplift event of 2000, *Journal of Volcanology and*
1930 *Geothermal Research*, **133**, 247-260.

1931

1932 Langella, A., Bish, D. L., Cappelletti, P., Cerri, G., Colella, A., de Gennaro, R., Graziano, S. F., Perrotta, A.,
1933 Scarpati, C. and de Gennaro, M., 2013. New insights into the mineralogical facies distribution of
1934 Campanian Ignimbrite, a relevant Italian industrial material, *Applied Clay Science*, **72**, 55-73.

1935

1936 Lima, A., De Vivo, B., Spera, F. J., Bodnar, R. J., Milia, A., Nunziata, C., Belkin, H. E. and Cannatelli, C.,
1937 2009. Thermodynamic model for uplift and deflation episodes (bradyseism) associated with magmatic–
1938 hydrothermal activity at the Campi Flegrei (Italy), *Earth-Science Reviews*, **97**, 44-58.

1939

1940 Lockner, D., 1993. The Role of Acoustic Emission in the Study of Rock Fracture, *International Journal of*
1941 *Rock Mechanics and Mining Sciences and Geomechanics Abstracts*, **30**, 883-889.

1942

1943 Lundgren, P., Usai, S., Sansosti, E., Lanari, R., Tesauro, M., Fornaro, G. and Berardino, P., 2001. Modeling
1944 surface deformation observed with synthetic aperture radar interferometry at Campi Flegrei caldera,
1945 *Journal of Geophysical Research*, **106**, 19355-19366.

1946

1947 Manconi, A., Walter, T. R. and Amelung, F., 2007. Effects of mechanical layering on volcano deformation,
1948 *Geophysical Journal International*, **170**, 952-958.

1949

1950 Manconi, A., Walter, T. R., Manzo, M., Zeni, G., Tizzani, P., Sansosti, E. and Lanari, R., 2010. On the
1951 effects of 3D mechanical heterogeneities at Campi Flegrei caldera, southern Italy, *Journal of Geophysical*
1952 *Research*, B08405, doi: 10.1029/2009JB007099.

1953

1954 Mogi, K., 1958. Relations between the eruptions of various volcanoes and the deformations of the
1955 ground surfaces around them, *Bull. Earthq. Res. Inst., Univ. Tokyo*, **36**, 99-134.

1956

1957 Nara, Y., Meredith, P. G., Yoneda, T. and Kaneko, K., 2011. Influence of macro-fractures and micro-fractures on permeability and elastic wave velocities in basalt at elevated pressure, *Tectonophysics*, **503**, 52-59.

1960

1961 Orsi, G., De Vita, S. and di Vito, M., 1996. The restless, resurgent Campi Flegrei nested caldera (Italy): constraints on its evolution and configuration, *Journal of Volcanology and Geothermal Research*, **74**, 179-214.

1964

1965 Peluso, F. and Arienzo, I., 2007. Experimental determination of permeability of Neapolitan Yellow Tuff, *Journal of Volcanology and Geothermal Research*, **160**, 125-136.

1967

1968 Plattner, C., Amelung, F., Baker, S., Govers, R. and Poland, M., 2013. The role of viscous magma mush spreading in volcanic flank motion at Kīlauea Volcano, Hawai'i, *Journal of Geophysical Research*, **118**, 2474-2487.

1971

1972 Ricci, T., Barberi, E., Davis., M. S., Isaia, R. and Nave, R., 2013. Volcanic risk perception in the Campi Flegrei area, *Journal of Volcanology and Geothermal Research*, **254**, 118-130.

1974

1975 Rolandi, G., Bellucci, F., Heizler, M. T., Belkin, H. E. and De Vivo, B., 2003. Tectonic controls on the genesis of ignimbrites from the Campanian Volcanic Zone, southern Italy, *Mineralogy and Petrology*, **79**, 3-31.

1978

1979 Rosi, M. and Sbrana, A., 1987. Phlegraean Fields, *Quaderni de "La Ricerca Scientifica": Consiglio Nazionale delle Ricerche Monograph 114*, Volume 9p. 175p.

1981

1982 Rutter, E., 1986. On the nomenclature of mode of failure transitions in rocks, *Tectonophysics*, **122**, 381-387.

1984

1985 Saccorotti, G., Petrosino, S., Bianco, F., Castelluccio, M., Galluzzo, D., La Rocca, M., Del Pezzo, E., Zaccarelli, L. and Cusano, P., 2007. Seismicity associated with the 2004–2006 renewed ground uplift at Campi Flegrei Caldera, Italy, *Phys. Earth Planet. Inter.*, **165**, 14-24.

1988

1989 Simmons, G. and Brace, W. F., 1965. Comparison of static and dynamic measurements of compressibility of rocks, *Journal of Geophysical Research*, **70**, 5649-5656.

1991

1992 Todesco, M., Rinaldi, A. P. and Bonforte, A., 2010. Modeling of unrest signals in heterogeneous hydrothermal systems, *Journal of Geophysical Research*, **115**, B09213, doi: 10.1029/2010JB007474.

1994

1995 Trasatti, E., Casu, F., Giunchi, C., Pepe, S., Solaro, G., Tagliaventi, S., Berardino, P., Manzo, M., Pepe, A., Ricciardi, G. P., Sansosti, E., Tizzani, P., Zeni, G. and Lanari, R., 2008. The 2004–2006 uplift episode at Campi Flegrei caldera (Italy): Constraints from SBAS-DInSAR ENVISAT data and Bayesian source inference, *Geophysical Research Letters*, **35**, L07308, doi:10.1029/2007GL033091.

1999

2000 Troiano, A., Di Giuseppe, Petrillo, Z., Troise, C. and De Natale, G., 2011. Ground deformation at calderas driven by fluid injection: modelling unrest episodes at Campi Flegrei (Italy), *Geophysical Journal International*, **187**, 833-847.

2003

2004 Troise, C., Castagnolo, D., Peluso, F., Gaeta, F. S., Mastrolorenzo, G. and De Natale, G., 2001. A 2D
2005 mechanical-thermal fluid-dynamical model for geothermal systems at calderas: an application to Campi
2006 Flegrei, *Journal of Volcanology and Geothermal Research*, **109**, 1-12.

2007
2008 Troise, C., De Natale, G., Pingue, F., Obrizzo, F., De Martino, P., Tammaro, U. and Boschi, E., 2007.
2009 Renewed ground uplift at Campi Flegrei caldera (Italy): New insight on magmatic processes and forecast,
2010 *Geophysical Research Letters*, **34**, DOI: 10.1029/2006GL028545.

2011
2012 Valentino, G. M., Cortecci, G., Franco, E. and Stanzione, D., 1999. Chemical and isotopic compositions of
2013 minerals and waters from the Campi Flegrei volcanic system, Naples, Italy, *Journal of Volcanology and*
2014 *Geothermal Research*, **91**, 329-344.

2015
2016 Vanorio, T., Virieux, J., Capuano, P. and Russo, G., 2005. Three-dimensional seismic tomography from P
2017 wave and S wave microearthquake travel times and rock physics characterization of the Campi Flegrei
2018 Caldera, *Journal of Geophysical Research*, **110**, B03201, doi:10.1029/2004JB003102.

2019
2020 Vinciguerra, S., Del Gaudio, P., Mariucci, M. T., Marra, F., Meredith, P. G., Montone, P., Pierdominici, S.
2021 and Scarlato, P., 2009. Physical properties of tuffs from a scientific borehole at Alban hills volcanic
2022 district (central Italy), *Tectonophysics*, **471**, 161-169.

2023
2024 Vinciguerra, S., Meredith, P. G. and Hazzard, J., 2004. Experimental and modeling study of fluid pressure-
2025 driven fractures in Darley Dale sandstone, *Geophysical Research Letters*, L09609,
2026 10.1029/2004GL019638.

2027
2028 Vinciguerra, S., Trovato, C., Meredith, P. G., Benson, P. M., Troise, C. and De Natale, G., 2006.
2029 Understanding the seismic velocity structure of Campi Flegrei caldera (Italy): from the laboratory to the
2030 field scale, *Pure and Applied Geophysics*, **163**, 2205-2221.

2031
2032 Wohletz, K., Civetta, L. and Orsi, G., 1999. Thermal evolution of the Phlegraean magmatic system,
2033 *Journal of Volcanology and Geothermal Research*, **91**, 381-414.

2034
2035 Wong, T.-f. and Baud, P., 2012. The brittle transition in rocks: a review, *Journal of Structural Geology*, **44**,
2036 25-53.

2037
2038 Zamora, M., Sartoris, G. and Chelini, W., 1994. Laboratory measurements of ultrasonic wave velocities in
2039 rocks from the Campi Flegrei volcanic system and their relation to other field data, *Journal of*
2040 *Geophysical Research*, **99**, 13553-13561.

2041
2042 Zhu, W., Baud, P., Vinciguerra, S. and Wong, T.-F., 2011. Micromechanics of brittle faulting and
2043 cataclastic flow in Alban Hills tuff, *Journal of Geophysical Research*, **116**, B06209,
2044 doi:10.1029/2010JB008046.

2045
2046 Zhu, W. and Wong, T.-F., 1997. The transition from brittle faulting to cataclastic flow: Permeability
2047 evolution, *Journal of Geophysical Research*, **102**, No. **B2**, 3027-3041.

2048
2049
2050